12-2021

Development of a Novel Strategy to Improve Checkpoint Immune Response in Pancreatic Cancer

Poornima Devi Shaji
The University of Texas Rio Grande Valley

DEVELOPMENT OF A NOVEL STRATEGY TO IMPROVE CHECKPOINT IMMUNE RESPONSE IN PANCREATIC CANCER

A Thesis

by

POORNIMA DEVI SHAJI

Submitted in Partial Fulfillment of the

Requirements for the Degree of

MASTER OF SCIENCE

Major Subject: Biochemistry and Molecular Biology

The University of Texas Rio Grande Valley

December 2021

DEVELOPMENT OF A NOVEL STRATEGY TO IMPROVE CHECKPOINT IMMUNE RESPONSE IN PANCREATIC CANCER

A Thesis
by
POORNIMA DEVI SHAJI

COMMITTEE MEMBERS

Dr. Subhash Chauhan

Chair of Committee

Dr. Sheema Khan

Committee Member

Dr. Murali Yallapu

Committee Member

December 2021

ABSTRACT

Shaji, Poornima Devi., Development of a Novel Strategy to Improve Checkpoint Immune Response in Pancreatic Cancer. Master of Science (MS), December, 2021, 84 pp., 6 tables, 29 figures, references, 55 titles.

Pancreatic Cancer is the 3rd lethal cancers in United States with a survival rate less than 5-7%. In advanced unresectable pancreatic cancer, treatment options are restrained to surgery because of its extreme aggressiveness. Immunotherapy, one of the current advanced treatments, has shown a promising response in other cancers. However, this therapy is limited to pancreatic cancer due to desmoplasia and fibrotic tumor microenvironment (TME).

Our superparamagnetic iron oxide nanoparticles (SPIONS) of curcumin (*Curcuma longa*, principal curcuminoid of turmeric) have potential ability to inhibit desmoplasia and tumor stroma with an increased bioavailability. This would soften up the tumors for therapies resulting in improved response to immune checkpoint therapies. Development of this novel combination therapy with (a) MUC13 conjugated SPION formulation of curcumin and (b) Checkpoint inhibitors PDL-1 (programmed death ligand 1), CTLA-4 (cytotoxic T lymphocyte antigen 4) has shown less tumor progression when compared to alone treatments in *in-vitro* and *in-vivo* studies. This could alleviate morbidity and mortality caused by the disease.

DEDICATION

The completion of my master's studies would not have been possible without the love and support of my family. My mother, Suma Shaji, my father, M. P. Shaji, my brother, Poojith M. S, wholeheartedly inspired, motivated, and supported me to accomplish this degree. Thank you for your love and patience. I would like to dedicate this to my father and mother, who has been a moral support and has let me follow my dreams.

ACKNOWLEDGMENTS

I will always be grateful to Dr. Subhash C. Chauhan and Dr. Sheema Khan, my thesis supervisors, for all their mentoring and advice. From research design, and data processing, to manuscript editing, they encouraged me to complete this process through their infinite patience and guidance. My thanks go to my dissertation committee members: Dr. Murali Yallapu, Dr. Subhash C Chauhan and Dr. Sheema Khan. Their advice, input, and comments on my thesis helped to ensure the quality of my intellectual work. I would also like to thank my colleagues from the Department of Immunology and Microbiology Ana Martinez Bulnes, Anyssa Rodriguez, Swathi Hola, Melida Flores Cantu, Nycol Cotto, Carlos Perez, Emmanuel Anning, Dr. Neeraj Chauhan, Dr. Anupam Dhasmana, Dr. Fnu Shabnam, Dr. Mohammed Sikander, Dr. Kyle Doxtater, Dr. Sudhir Kotnala for their support and help in the project. My heartfelt gratitude to Dr. Sreejith Parameswara Panicker, Department of Zoology, University of Kerala, my previous mentor for his guidance at every stage of my research. His mentorship with prompt inspirations, timely suggestions, enthusiasm, and dynamism have enabled me to accomplish master's from University of Texas Rio Grande Valley. Thanks to Anitha Narayanan and Santhosh Mukingal for their valuable guidance and timely help. The work was supported by UTRGV grant support (35000459) to Dr. Sheema Khan and NIH R01 CA206069 to Dr. Subhash C. Chauhan and Dr. Sheema Khan.

TABLE OF CONTENTS

LIST OF TABLES

Page

LIST OF FIGURES

Page

CHAPTER I

INTRODUCTION

1. Statement of The Problem

Pancreatic cancer is currently ranked 3rd cause of death in United States and 7th in world. This year, an estimate of 60,430 new cases have been reported with an estimated death of 48,220. If diagnosed and screened early there is a better chance of a person to survive up to 5 years. Based on the data from SEER 18 2011–2017, the 5year relative survival rate for pancreatic cancer increased to 10.8%(SEER, 2021). The short lifespan of the pancreatic cancer patient is contributed to lack of markers for early detection, screening programs and aggressiveness of the tumor. The aggressiveness of pancreatic tumor makes it hard to treat and underlay different levels of therapeutic resistance.

In most cases, pancreatic cancer is diagnosed in the advanced or metastasize stages which makes it less effective to localized therapies such as surgery. ABRAXANE in combination with gemcitabine is the current first line treatment for pancreatic ductal adenocarcinoma (PDAC) (Saif, 2013) . Chemotherapy may have some benefits, but most approaches to improve the current regimens is constantly failing in advanced clinical trials. Immune checkpoint blockade therapy has become a major emerging weapon in fighting many cancers and it has been recognized as a key strategy to control the progression of malignant tumors. But immunotherapies, including immune checkpoint inhibitors have had limited success in treating PDAC due to its low antigenicity and immunogenicity.

PDAC's low antigenicity is a result of a low frequency of tumor associated antigens (TAA), low tumor mutational burden (TMB) and most importantly increased fibrotic tumor stroma, limiting the successful checkpoint immunotherapy response. Therefore, there is a need of understanding and implementing a combined approach that can target tumor stroma and improve immune response in pancreatic cancer patients.

2. Statement of The Purpose

In the proposed study, we are developing a novel antibody mediated nanodrug formulation that can inhibit tumor stroma and improve immune response in pancreatic patients. Here, we are using Curcumin (CUR), a naturally occurring polyphenol derived from the root of *Curcuma longa* (Aggarwal, Sundaram, Malani, & Ichikawa, 2007). My mentor lab (Khan et al., 2019) has shown effective delivery of curcumin when encapsulated within super paramagnetic iron oxide nanoparticle (SPION-CUR). Curcumin is a non-toxic, bioactive anti-inflammatory or anti-cancer agent that can target tumor microenvironment by inhibiting tumor stroma via suppression of sonic hedgehog (SHH) pathway, an oncogenic CXCR4/CXCL12 signaling axis and may inhibit cell invasion and EMT via the IL□6/ERK/NF□κB axis (Khan et al., 2019; Li et al., 2020). This formulation is conjugated with antibody to mucin, MUC13, which is highly expressed in PDAC. The purpose of MUC13 conjugation is to aim for pancreatic tumor specific delivery of the therapeutics.

Our purpose is to target tumor stroma using a novel antibody mediated SPION-CUR formulation in a combined approach. This antibody mediated targeted therapy can deliver curcumin most effectively and reduce tumor stromal inhibition which can improve patient's outcome to checkpoint inhibitor immunotherapy in pancreatic cancer. The combination therapy includes (a) MUC13 conjugated super paramagnetic iron oxide nanoparticle of curcumin

(SPION-Cur) formulation along with (b) Immune checkpoint inhibitors (PDL1 and CTLA4). The efficacy of nano formulation was studied using pancreatic cell lines and combined targeted therapy was performed in female C57BL/6J black mice.

CHAPTER II

REVIEW OF LITERATURE

1. Pancreatic Cancer

1.1 Statistics

Globally, pancreatic cancer accounts for 496,000 new cases with an estimated deaths of 466,000 in 2020 (GLOBOCAN 2020 estimates) and is the 7th leading cause of cancer death. Rate of incidence of pancreatic cancer is 4 to 5- fold higher in the Human Development Index countries like Europe, Northern America, and Australia/New Zealand. In a study done with 28 European countries, it has been projected that pancreatic cancer will overtake breast cancer as third leading cause of death by 2025 (Sung et al., 2021). Based on the data from SEER 18 2011–2017, the 5year relative survival rate for pancreatic cancer increased to 6 to 10.8% (SEER, 2021).

The American Cancer Society estimated that in 2021, about 60,430 people (31,950 men and 28,480 women) will be diagnosed with pancreatic cancer and about 48,220 people (25,270 men and 22,950 women) will die from pancreatic cancer. According to a data from 2018, an estimation of 83,777 people is living with pancreatic cancer in the United States. The average likelihood of a person getting pancreatic cancer in some point of their lifetime is 1 in 64. Approximately 1.7 percent of women and men are likely to be diagnosed with pancreatic cancer

based on 2016–2018 data. But the person's chance of getting pancreatic cancer may depend on certain risk factors(SEER, 2021).

1.2 Risk Factors

Factors that can increase the risk of pancreatic cancer are older age (as most people are diagnosed after 65), smoking, alcohol consumption, diabetes, chronic inflammation of the pancreas, or pancreatitis, family history of genetic syndromes that can increase cancer risk (including a BRCA2 gene mutation, lynch syndrome and familial atypical mole malignant melanoma syndrome), family history of pancreatic cancer, obesity, industrial chemical exposures (Capasso et al., 2018). Additional risk factors are gender (more common in men than in woman), ethnicity (African Americans are more likely to develop pancreatic cancer than whites, Asians or Hispanics) (Hu et al., 2021).

African Americans (AA) have highest incidence rate between 28% and 59% higher than other racial groups. The mortality rate for AA is 13.3 per 100,000 people, while for whites is 11.0 per 100,000(American Cancer Society, 2019a). Incidence of pancreatic cancer and increased smoking and alcohol consumption among African Americans indicates lifestyle risk rather than genetics. Risk of getting pancreatic cancer is double among people who smoke than non-smokers (Mocci et al., 2021).

1.3 Pathogenesis

Pancreatic cancer affect pancreas, a 6 inches long organ situated across the back of abdomen behind the stomach. Pancreas produces digestive juices and hormones that regulate blood sugar. Anatomically pancreas is divided into three regions: head, body, and tail. Pancreatic carcinoma is described as uncontrolled growth of malignant cells. The most common type of

pancreatic cancer is pancreatic ductal adenocarcinomas (PDAC), about 95% tumor arises from uncontrolled growth of exocrine cells. They tend to occur in the head of the pancreas and may grow quickly. About 10% of pancreatic cancer are endocrine or Islet cell cancer. These tend to be more slower growing tumor that is in the body or tail of the pancreas. Other types of rare pancreatic cancers is lymphoma, sarcoma, acinar, solid and pseudopapillary cancers (American Cancer Society, 2019c).

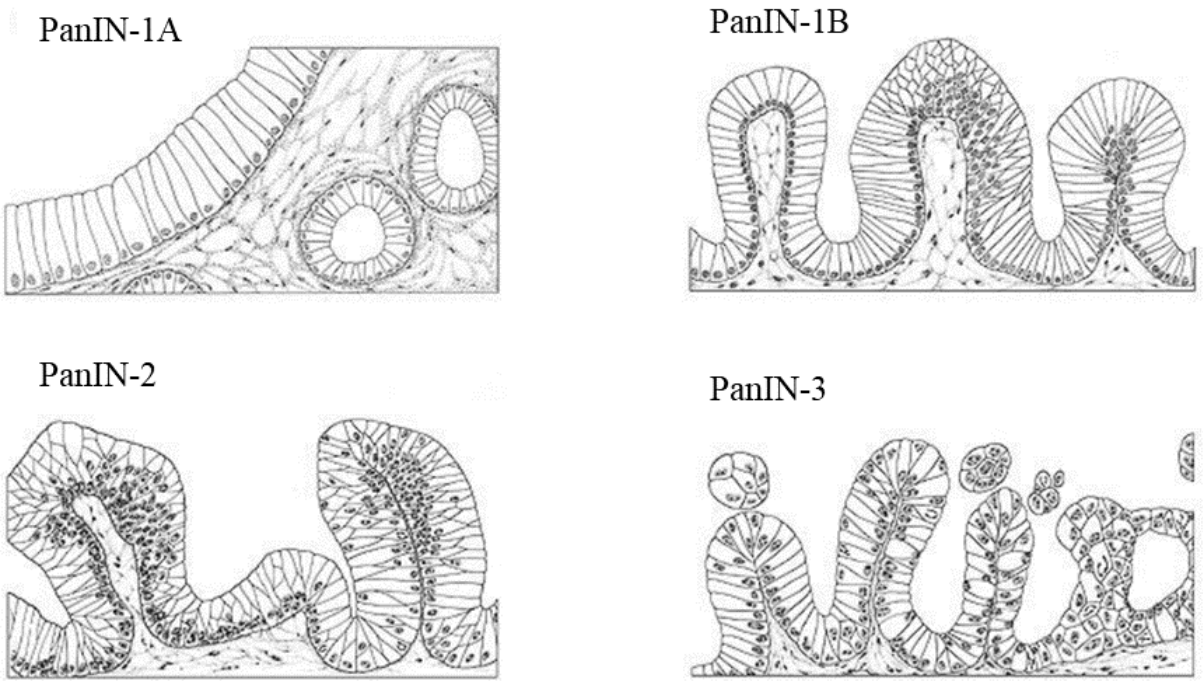

Fig.1. Pancreatic ductal lesion classification into PanIN-1A, PanIN-1B, PanIN-2, PanIN-3 (Johns Hopkins Medicine Pathology, 2021)

The precancerous lesions are classified into three, smaller lesions are called pancreatic intraepithelial neoplasia (PanIN), the larger lesions are called intraductal papillary mucinous neoplasms (IPMNs) and Mucinous cystic neoplasms (MCN). In which, the most know precursor for PDAC is Pancreatic Intraepithelial Neoplasia (PanIN). PanINs are divided into 4 subgroups

based on the condition of epithelial atypia and amount of mucin appearance. PanIN-1A and PanIN-1B (low grade), PanIN-2 (intermediate-grade), PanIN-3 (High-grade) (Hruban et al., 2001) (Fig.1.).

Stages of pancreatic cancer are divided based on tumor size and whether tumor has spread to nearby structures. Stage I and II referred to a localized tumor which can be diagnosed by preoperative imaging after surgery. In stage I (less than or equal to 2 cm) these are small localized and in stage II (greater than 2 cm) tumors are seen with or without lymph node involvement. This stage of pancreatic cancer can be considered for resectable surgery. In stage III tumors are wrapped around superior mesenteric veins and cannot be surgically removed as it has been spread to arteries. This stage is often called as locally advanced. In Stage IV cancer has spread to other organs especially to liver and inner lining of abdominal cavity, the lungs, lymph nodes and more rarely bones. The chance of undergoing surgical resection is very less at stage IV (Malhotra, Ahn, & Bloomston, 2015).

1.4 Diagnostic and Treatment

The diagnostics play an important role in early recovery of cancer. Unfortunately, pancreatic cancer is diagnosed usually at advanced stages due to lack of awareness, diagnostic markers, and proper screening programs. Diagnostics for pancreatic cancer includes physical and medical examination, Imaging tests (MRI, PET, Endoscopic Ultrasound and CT scans), Cholangiopancreatography, Angiography, blood tests, Biopsy. Cholangiopancreatography looks at pancreatic and bile ducts to see if they are blocked, dilated, or narrowed. There are three types of cholangiopancreatography, they are Endoscopic retrograde cholangiopancreatography (ERCP), Magnetic resonance cholangiopancreatography (MRCP), Percutaneous transhepatic cholangiography (PTC). Tumor markers that may detect pancreatic cancer are CA 19-9,

Carcinoembryonic antigen (CEA). These markers are not accurate may vary in pancreatic patients. In patients with high level of CA 19-9 or CEA, these markers could be used to check the effectiveness of the treatment (American cancer Society, 2020b). There is an unmet need of a proper diagnostic marker that can detect the pancreatic cancer in the early stages which can help in faster recovery.

Treatment options may vary with stages of pancreatic cancer. In most cases, surgery is preferred in localized tumors followed by chemotherapy and radiation. If diagnosed early pancreatic cancer can be treated by two kinds of surgeries- Pancreatectomy (Distal and total) and Whipple procedure. Whipple procedure is the most common surgery used to remove a cancer from the head of pancreas. During this procedure surgeon removes head of the pancreas and maybe some parts of body of the pancreas. The remaining portion of bile duct and pancreas is stitched, so that digestive enzyme can still go to small intestine (American Cancer Society, 2019b). The most common and approved chemo drugs used as adjuvant and neoadjuvant chemo are Gemcitabine (Gemzar), 5-fluorouracil (5-FU), Oxaliplatin (Eloxatin), Albumin-bound paclitaxel (Abraxane), Capecitabine (Xeloda), Cisplatin, Irinotecan (Camptosar) (American Cancer Society, 2020a). FOLFIRINOX, is the most common drug combination (FOL = Leucovorin Calcium (Folinic Acid), F= Fluorouracil, IRIN= Irinotecan Hydrochloride, OX= Oxaliplatin) used to treat metastatic pancreatic tumor (National Cancer Institute, 2018)

These therapies are used as standard care in pancreatic cancer but due to aggressiveness and therapeutic resistance of the disease, there is an urgent need for the development of advanced alternative treatment options that can focus on the tumor chemo resistance and cure the disease (Oberstein & Olive, 2013). Currently, targeted therapies and immunotherapies are under clinical

trials with a focus on therapeutic implication on tumor stroma (Adamska, Domenichini, & Falasca, 2017).

2. Pancreatic Tumor Immune Microenvironment

2.1 Immune Cells and Tumor Immune Surveillance

In a progressing tumor, neither the tumor nor the tumor Immune microenvironment (TIME) is constant. The studies have shown that the reciprocal interactions of tumor associated immune cells and stromal cell types are evolving with tumor growth. Tumor cells have developed several strategies that can mimic peripheral immune tolerance to escape tumor immune surveillance. The tumor immune surveillance is an immune defense mechanism to identify and destroy abnormal cells, most likely prevents, or curbs the growth of cancerous cells or precancerous cells (Swann & Smyth, 2007). During the progression of tumor, these immune cells are present around and are known as tumor-infiltrating lymphocytes (TILs). People with high TILs are shown to do better immune response compared to people with low TILs. TILs include innate immune cells (natural killer cells, macrophages, neutrophils, dendritic cells, mast cells, eosinophils, basophils) and adaptive immune cells (T cells and B cells)(Binnewies et al., 2018). In addition to TILs the tumor microenvironment (TME) consists of stromal cells such as fibroblasts, endothelial cells, pericytes, and mesenchymal cells (Grivennikov, Greten, & Karin, 2010).

Tumor immune microenvironment has relatively no or less cytotoxic lymphocytes (CTLs), these are termed as infiltrate-excluded TIMEs (I-E TIMEs). I-E TIMEs consists of high tumor associated macrophages (TAM) and promote tumor growth, angiogenesis, invasion and metastasis (Binnewies et al., 2018). In most of the epithelial cancers such as melanoma,

colorectal cancer, pancreatic ductal adenocarcinoma (PDAC) tumor associated macrophage (Ly6Clo F4/80hi) prevent the cytotoxic infiltrates towards tumor environment (Beatty et al., 2015). Adaptive immune cells such as matured T cells are further classified based on their co-receptors and effector functions. They are $CD8^+$ effector T cells, $CD4^+$ helper T cells (which consists of Th 1, Th2, Th17), T regulatory cells (T reg) and natural killer T (NKT) cells (Binnewies et al., 2018).

Cytotoxic $CD8^+$ T cells targets and binds to antigen peptides associated with major histocompatibility complex class I (MHC I), present on the surface of antigen presenting cells (APCs) or tumor cells. Meanwhile helper $CD4^+$ T cells binds to antigen peptides associated with MHC II class, present on APCs. Activated helper CD4+ T cells (Th 1) then secretes proinflammatory cytokines (IL-2, TNF-α, and IFN-γ) and induces anti-tumoral activity of macrophages and NK cells. Regulatory $CD4^+$ T cells (T reg) consist of two important variants FOXP3+ Treg cells and FOXP3. The function of $CD4^+$ Treg is to stop the T-cell mediated immune response at the end of an immune reaction. Other types of T cell are memory T cells, upon re-exposure to related antigen they expand to large number of effector cells $CD4^+$ and $CD8^+$.

T cells play dual role in cancer progression, in early stages of tumor development it secretes Th-1 cytokines (IFN-γ, IL-2, and IL-12), recruit NK cell and control the tumor progression. In the later stage tumor outgrows and starts to metastasis by escaping immune surveillance. As a result, regulatory CD4+ T cells (Tregs) are recruited that oppose anti-tumor immune cells from destroying them. High level of CD4+ T cells (Tregs) is associated with poor prognosis in most of the cancers. One of the mechanisms in which the cancer cells escape immune surveillance is through hampering immune checkpoint function. During immune

response these immune checkpoints regulate signals and protect normal cells from getting attacked. Cancerous cells dysregulate this immune checkpoint proteins and escape from immune attack. There are two types of immune checkpoint signals, co- stimulatory signals (such as CD28, ICOS, and CD137) and co- inhibitory signals (such as PD1, PDL-1, CTLA-4, and VISTA) (Pardoll, 2012). Immune checkpoint therapies use agonist of co- stimulatory signals or antagonist of co-inhibitory signals to revert and improve immune defense.

2.2 Immune Checkpoint Therapies in Pancreatic Cancer

The most common immune checkpoint therapy used in the treatment of solid cancers (such as melanoma, colon cancer and pancreatic cancer) are antagonists of co-inhibitory signals. These inhibitory drugs, such as anti-PD1, anti- PDL-1, anti-CTLA-4 block the immune checkpoints and may reprogram immune cells to destroy cancer cells. Examples of FDA approved Immune checkpoint inhibitors for treatment of other cancers are Ipilimumab (Yervoy®) that blocks a checkpoint protein called CTLA-4, Pembrolizumab (Keytruda®) and nivolumab (Opdivo®) which target checkpoint protein called PD-1, and Atezolizumab (Tecentriq®) targets PDL-1 (Yoon, Jung, & Moon, 2021b).

FDA recently approved use of anti-PD1 (pembrolizumab and nivolumab) immunotherapy for solid cancer with MSI-h or mismatch repair deficiency (Boyiadzis et al., 2018; Yoon, Jung, & Moon, 2021a). Other immune checkpoint inhibitors are in clinical trials. However, this therapy is limited in pancreatic cancer due to desmoplasia and fibrotic tumor microenvironment. Therefore, development of newer strategies to enhance immunotherapy is required, Wherein, tumor stroma can be depleted using combined drugs for improved tumor response to immunotherapies.

2.3 Factors Limiting the Success of Checkpoint Therapy in Pancreatic cancer

Pancreatic tumor microenvironment is a hot spot for fibrotic stroma that contains a variety of cells (stellate cells, pan-endothelial cells, and infiltrating immune cells such as MDSC, Treg cells, and tumor-associated macrophages) and extracellular matrix (ECM) components with blood vessels and nerves. The main reason for the failure of advanced therapies in pancreatic cancer is because of its complex tumor microenvironment, especially due to desmoplastic PDAC stroma. Cancer associated fibroblast (CAFs), activated stellate cells are the main source of ECM and collagen that form desmoplastic PDAC stroma (Apte, Wilson, Lugea, & Pandol, 2013). This stromal core consisting of CAFs, infiltrating immune cells, blood vessels, and ECM components (include collagen, fibronectin, proteoglycans, hyaluronic acid) and enzymes are responsible for chemoresistance (Feig et al., 2012). Other factors limiting the success of immune checkpoint inhibitor therapy are increased toxicity, impaired antigen recognition and T cell activation, low TILs, low mutational burden (TMB) to the complex interactions between tumor cells, heterogeneity of desmoplastic stroma and dominance of immunosuppressive cells (TAMs, CAFs, MDSCs and T regs) (Young, Hughes, Cunningham, & Starling, 2018). These immunosuppressive inflammatory cells can promote the migration of pancreatic cancer through the CXC motif chemokine ligand (CXCL)-CXC chemokine receptor (CXCR) axis (Lafaro & Melstrom, 2019). These factors make the pancreatic cancer insusceptible to monotherapies.

3. Approaches for Increasing Effectiveness of Immune Checkpoint Therapy

3.1 Combined Immune Therapies in Pancreatic Cancer

The failure of monotherapy in PDAC could be overcome by combination therapies. The combination can be with immunotherapeutic agents, targeted therapies, stromal modulating

agents, microbial ablation, chemotherapy, radiotherapy, chemoradiotherapy, or multi-way combination therapies (Yoon et al., 2021a). In advanced pancreatic cancer, studies have shown better outcome in the combination therapy. For example, gemcitabine with immune checkpoint inhibitors ipilimumab (Kamath et al., 2020), nab-paclitaxel and nivolumab (Wainberg et al., 2020) have shown better response when compared to gemcitabine alone. Similarly, gemcitabine along with nab-paclitaxel and pembrolizumab in metastatic pancreatic cancer showed better result when compared to single therapy (Weiss et al., 2018). Other combination is along with vaccine GVAX and immunotherapy (Wu et al., 2020). Combination therapies are currently under clinical trials, so far there is no FDA approved combination therapy for pancreatic cancer (ClinicalTrials.gov).

3.2 Targeting Stroma

The dense tumor stroma and tumor microenvironment are the key contributors for the PDAC aggressiveness. Targeting of tumor stroma ablates the physical barrier caused by CAF, immune suppressor cells, ECM includes collagen, fibronectin, proteoglycans, hyaluronic acid. Curcumin (CUR) is a naturally occurring polyphenol derived from the root of Curcuma longa. It has demonstrated potent anti-cancer and cancer prevention activity in a variety of cancers (Aggarwal et al., 2007). Previous reports have demonstrated the tremendous efficacy of curcumin to inhibit desmoplasia and tumor stroma (Khan et al., 2018). Therefore, curcumin can be a good candidate for improving immunotherapies by targeting tumor stroma (Khan et al., 2019). Clinical translation of curcumin has been significantly hampered due to its extensive degradation, suboptimal pharmacokinetics, and poor bioavailability. This could be overcome by the application of nanotechnology where curcumin is encapsulated within a nano formulation (M. M. Yallapu et al., 2013). Studies have shown tremendous increase in the uptake of curcumin,

superparamagnetic iron oxide nanoparticle of curcumin (SPION-CUR) in pancreatic cancer (Khan et al., 2019).

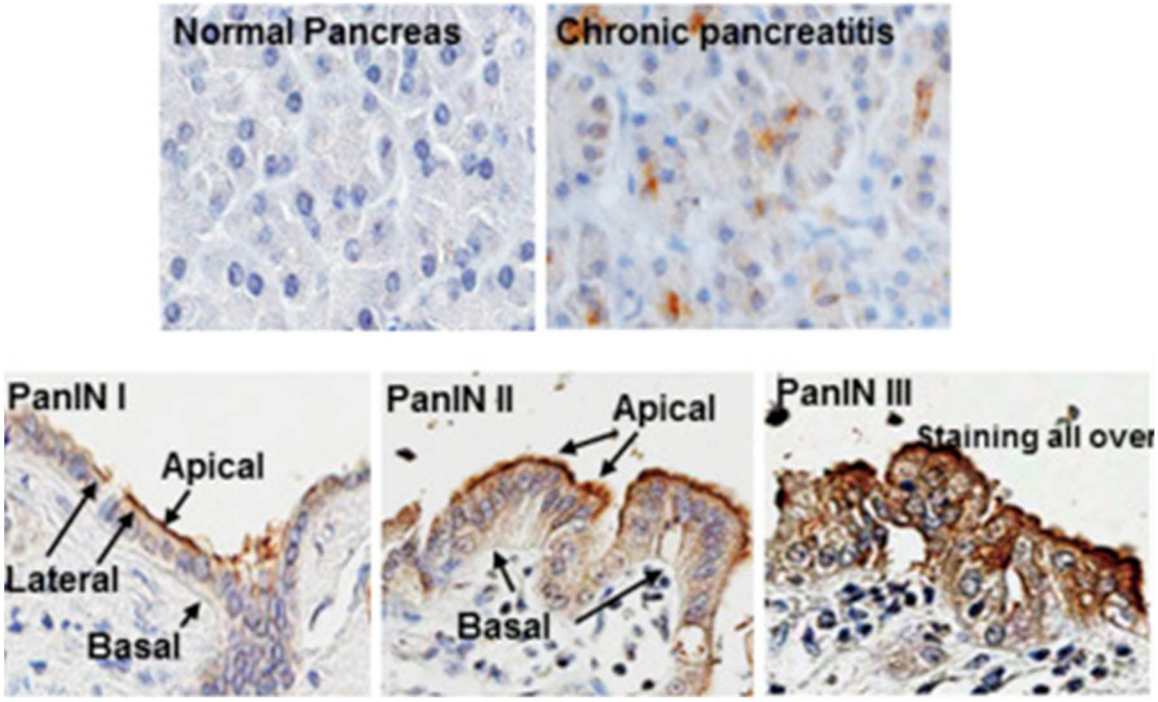

Fig. 2. Expression of MUC13 in pancreatic cancer. MUC13, is aberrantly expressed in the chronic pancreatitis, PanINs (I-III) but not in normal pancreas (brown) (Khan et al., 2018)

MUC13, a mucin glycol protein aberrant expression in pancreatic tumors (Fig. 2.) has a tremendous tumor targeting ability and may serve as an excellent target for Pancreatic cancer treatment (Khan et al., 2014; Khan et al., 2018). Interestingly, studies have shown MUC13 mAb may have a potential ability to target towards the pancreatic tumor environment and deliver the drug effectively (Khan et al., 2014; Khan et al., 2018; Mashayekhi et al., 2021).

3.3 Nanoparticle Mediated Delivery of Drugs

Efficacy of anticancer drugs such curcumin (Li et al., 2020), Amd3100 (Biasci et al., 2020) that target stroma is hampered due to systemic degradation, poor bioavailability, unsatisfactory pharmacokinetic profile, drug resistance and side effects (M. M. Yallapu et al., 2013). This could be resolved using nanoparticle which can target tumors efficiently with the help of unique characteristics, such as the "Enhanced Permeation and Retention" (EPR) effect. The nano size of particles can increase surface-area-to-volume ratio which leads to higher surface attachment capacity (Peer et al., 2007). These nanocarriers has prolonged systemic circulation that can improve delivery of drug with an increased bioavailability. Nanotechnology deals with materials and devices in a nanometer scale of 1-100 nm in dimension and play an important role in targeted delivery in cancer therapy. One such nano formulation is super paramagnetic iron oxide nanoparticle (SPION) which are nontoxic, biocompatible, biodegradable and easily internalized in cells (Khan et al., 2019; M. M. Yallapu et al., 2013). Studies have shown nano drug loaded curcumin has more bioavailability, anti-inflammatory, and anticancer properties (Khan et al., 2019; M. M. Yallapu et al., 2013).

3.4 MUC13 - As a Unique Target for Pancreatic Cancer

The poor survival rate in pancreatic cancer is due to the lack of early detection and poor prognostic markers. Recent studies in pancreatic cancer have shown high expression of a glycosylated mucin protein known as MUC13,100% in pancreatic intraepithelial neoplasia (PanIN lesions) and 94% in pancreatic adenocarcinoma (PDACs). In pancreatic cancer cells, the TR domain of mucin glycoprotein, MUC13 is aberrantly hypo-glycosylated compared to normal pancreatic epithelial cells and this may serve as an excellent target for Pancreatic cancer treatment (Maher, Gupta, Nagata, Jaggi, & Chauhan, 2011). Studies have shown aberrant

expression and localization of MUC13 in PanCa samples using anti-MUC13 mAb (Chauhan et al., MCT; 2012). Additionally, MUC13 expression influences tumorigenesis via alterations of multiple signaling pathways. Therefore, antibodies against the TR domain will preferentially target tumor cells due to higher/aberrant expression, all over the cell surface and glycosylation of MUC13 in cancer cells compared to normal cells. Previously published article from our lab revealed that normal pancreatic duct has very low or no expression of MUC1where as late-stage PanINs displayed significant expression of MUC13. Increasing expression of MUC13 was identified with progression of PanINs-I to PanIN-III (Fig.2.). Researchers have shown significantly higher expression of MUC13 in advance stage of IPMNs. The study of MUC13 expression provides significant information regarding its influence on molecular processes that are supportive of interactive TME that lead to drug resistance/metastasis (Khan et al., 2018). The studies support the use of MUC13 antibodies as a diagnostic/ prognostic test and could be a good target for the delivery of drug in pancreatic cancer.

CHAPTER III

GENERATION, CHARACTERIZATION AND FUNCTIONAL CHARACTERISTICS OF A NOVEL MUC13 CONJUGATED SPION NANOFORMULATION FOR PANCREATIC CANCER

1. BACKGROUND

Pancreatic cancer, also known as pancreatic adenocarcinoma, remains a highly lethal human malignancy due to a failure of effective adjuvant therapies (Siegel, Miller, & Jemal, 2016). The key factors that limit the most effective treatments are lack of early detection, high chance of metastasis, recurrence even after surgical resection, chemoresistance due to desmoplasia and stromal factors (Zhang, Sanagapalli, & Stoita, 2018). Curcumin (CUR) is a naturally occurring polyphenol derived from the root of *curcuma longa.* It has demonstrated potent anti-cancer and cancer prevention activity in a various cancer. Previous reports from my mentor's lab and the ones published by others have demonstrated the tremendous efficacy of curcumin to inhibit desmoplasia and tumor stroma (Khan et al., 2019; Qu, Wang, Meng, & Wang, 2018; Teng et al., 2020). These studies indicate the potential of curcumin in improving immunotherapies via targeting tumor stroma.

Clinical translation of curcumin has been significantly hampered due to its extensive degradation, suboptimal pharmacokinetics, and poor bioavailability. Therefore, in order to overcome its limitations to clinical translation, previous work from mentor's Lab have demonstrated the development of a novel super paramagnetic nanoparticles (SPION) for the

efficient delivery of curcumin (Khan et al., 2019; M. M. Yallapu et al., 2013; Murali M Yallapu et al., 2011). Magnetic nanoparticle formulations for drug delivery that have previously been generated by others have demonstrated poor therapeutic efficacy for cancer treatment due to the high particle size in suspension, loss of magnetization and inefficient internalization in the target cells. In contrast, our unique magnetic nanoparticle-based systems are stable and highly efficient for drug delivery applications. Our lab has demonstrated that our uniquely engineered SPIONs have multifunctional properties, including enhanced MRI properties compared to conventional MNPs (Murali M Yallapu et al., 2012; Murali M Yallapu et al., 2011).

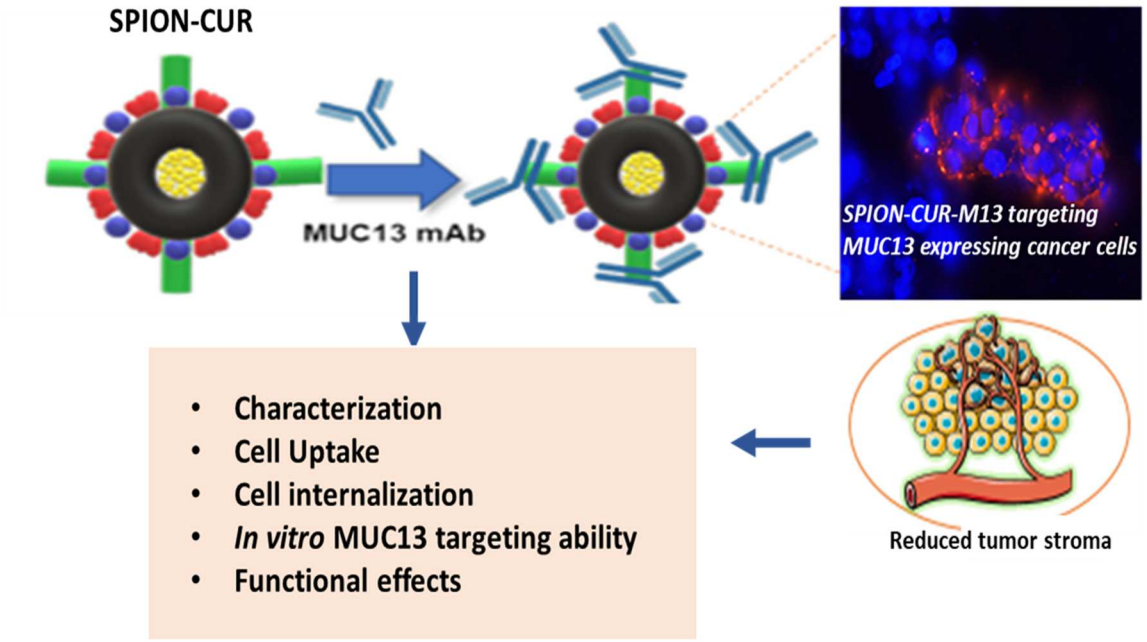

Fig. 3. Schematic representation of the study in Chapter III. Generation of SPION-CUR-MUC13 formulation, investigate its efficacy to internalize in the cells and demonstrate its targeting ability to detect Muc13 expressing cells.

In this study, in order to achieve pancreatic tumor specific delivery of curcumin, we have conjugated the SPION formulation with our in-house generated MUC13 monoclonal antibody (Fig. 3.). MUC13 is a transmembrane glycoprotein, that is aberrantly expressed in pancreatic cancer and progressively increases with the increased tumor aggressiveness (Khan et al., 2018). This gives it an ideal tumor targeting ability and suggests that it may serve as an excellent target for pancreatic cancer treatment. Therefore, in this chapter III, following three objectives are accomplished, ***(i)*** generation and characterization of MUC13 conjugated SPION-Curcumin (SP-CUR-M13), ***(ii)*** investigate its ability to internalize efficiently into cells and demonstrate its MUC13 targeting ability, and ***(iii)*** investigate the functional efficacy of the formulation in cells with the help of different cell based *in vitro* assays.

2. MATERIALS AND METHODS

2.1 Chemicals, Reagents, and Antibodies

All chemicals and reagents were purchased from Sigma Aldrich Corporation and cell culture wares were purchased from Corning life sciences. TRIzol reagent (catalog number # AM 9738) were purchased from Life technologies. XenoLight D-Luciferin Potassium Salt (PerkinElmer Health Sciences, Inc. catalog number #122799). The primary antibodies, anti-PDL-1 (abcam catalog number #13684), anti-CTLA-4 (abcam catalog number # ab237712), MUC13 (in house generated).

2.2 Culture of Pancreatic Cancer Cells

Human pancreatic cancer cells HPAF, Panc1, AsPC-1 were used to study the efficacy of SPION-CUR nano formulation. Muc13 null and Muc13 positive cell lines of Panc-1 was

generated in our lab to determine the internalization and targeting efficacy of SPION-CUR-MUC13 nano formulation. Further, for *in-vitro* and *in-vivo* studies we have generated lentiviral expressing KPC luciferase mouse cell line. KPC cell line has been generated from Pdx1cre; LSL-KrasG12D; LSL-Trp53R172H (KPC) mice. The KPC mice recapitulates the disease progression seen in human, such as initiation of PanCa with mPanINs, followed by progression to invasive adenocarcinoma, and subsequent metastasis into distant organs. The cells carry mutation in transformation related protein such as p53 gene (TP53R172H), and KRAS gene (KRASG12D). Therefore, KPC cells provide unique opportunity to investigate the targeting efficacy and treatment outcomes of our SPION-CUR-MUC13 formulation. KPC cells were cultured using cell specific culture media F12/DMEM and RPMI (Gibco), respectively, which was supplemented with 10% fetal bovine serum (Gibco) and antibiotic/antimycotic solution at 37 °C in a humidified atmosphere (5% CO2 and 95%air atmosphere). Luciferase cells were routinely tested and added with puromycin to make it stable.

2.3 Design and Preparation of SPION-CUR formulation for Pancreatic Cancer

Superparamagnetic iron oxide nanoparticles were synthesized by co-precipitating Fe2+ and Fe3+ iron salts in presence of ammonia under nitrogen atmosphere. The Fe2+ and Fe3+ iron salts were reduced by ammonia, in the presence of 200 mg β-cyclodextrin (β-CD) and 250 mg Pluronic polymer [(F127, poly (ethylene-co-propylene glycol)] and the resulted formulations developed in the form of magnetite (negatively charged with negative zeta potential values). The CD was purchased from Sigma Aldrich, St. Louis, MO (catalog number # C4805), which provides hydrophilic units (−OH) and hydrophobic cavity for binding to iron oxide nanoparticles and loading anti-cancer drugs, respectively (M. M. Yallapu et al., 2013; Murali M Yallapu et al., 2011). F127 provides additional hydrophilicity and stability to overall formulation. For example,

to load CUR in the SPIONs, 1 mg CUR in 200 µl acetone was added dropwise to 2.75 ml of an aqueous dispersion of SPIONs (10 mg).

The curcumin-loaded nanoparticles were washed three times by resuspending them in water and separated with the help of magnets. These drug-loaded nanoparticles were dispersed in 2 ml sterile phosphate buffered saline (1X PBS) solution and stored in a refrigerator until use. For in vitro and in vivo experiments, SPION-CUR 2 mM formulation was employed. 2 mM SPION-CUR was used as a master stock which was further diluted to achieve 2.5 µM, 5 µM, 10 µM, 15 µM and 20 µM equivalent curcumin concentration for in vitro studies.

2.4 MUC13 Labelling of SPION-CUR

Conjugation of SPION-CUR with MUC13 antibody was done in two steps. In first step, surface moiety on SPIONs is activated, 1 mg/ml SPION-CUR (considering the weight of curcumin) with 10 mM sodium bicarbonate reaction buffer (pH 8). The activated SPION is then mixed with 1mg of PEG succinimidyl ester linker, MW 5000 (NANOCS, NHS-PEG-NHS) in a stirring plate for an hour. The unreacted linker was removed by washing using magnet and activated NHS linked SPIONs were again suspended in PBS. In second step, 100 µg of MUC13 was slowly added at 4□ for 18hrs to generate MUC13 targeted SPIONs. The unconjugated MUC13 was removed by washing using magnet done in room temperature for 1hr.

2.5 Determination of Particle Size and Zeta Potential of SPION Formulation

The hydrodynamic nanoparticle size and zeta (ζ) potential of SPION and SPION-CUR were determined by the dynamic light scattering (DLS) principle using Zetasizer (NanoZS, Malvern Instruments, Malvern, UK). To measure the particle size 150µL of 10mg/ml nanoparticle suspension was added to 3ml of water and probe sonicated using VirSonic-Ultrasonic Cell

Disrupter 100 128 (VirTis, Gardiner, NY) for 15 seconds. For ζ-potential measurement, 50 µl of 10 mg/ml nanoparticle suspension was added to 1 ml of 1X PBS were used.

2.6 Internalization of Nanoparticle Formulation in Pancreatic Cancer Cells

2.6.1 Prussian Blue Staining for uptake of formulation

Prussian blue staining was used to determine the cellular uptake of SPION formulations in the pancreatic cancer cells; AsPC-1 and KPC. Cells were seeded in 6 well plate with 0.8 million cells per well and next day cells were treated with SPION (control), Cur (15 µM), and SPION-CUR (15 µM), SPION-CUR (20 µM) in ASPC-1 cell line; and SPION (control), Cur (15 µM), SPION-CUR (10 µM) and SPION-CUR (15 µM), SPION-CUR (20 µM) in KPC cell line. After 6hrs, cells were washed (with 1X PBS), fixed (with methanol), and incubated with a mixture of 2%potassium ferrocyanide, 2% hydrochloric acid (30min) (Murali M Yallapu et al., 2012).

2.6.2 Confocal Immunofluorescence Assays for cell internalization

Internalization of SPION-CUR was evaluated in pancreatic cancer AsPC-1 cell line. Cells were treated with SPION-CUR nanoparticle formulation and analyzed for internalization using immunofluorescence and imaged through confocal microscopy. Cells were treated with for 18h with SPION-CUR (15 µM). After 18hrs of incubation, treatment was terminated and fixed with 4%PFA for obtaining immunofluorescence image through microscopy. Curcumin has strong fluorescence as biocompatible probe for bio-imaging.

Internalization efficacy of SPION-Anti-MUC13 was checked in MUC13 null and MUC13 positive Panc-1 cells. 90,000 cells per well of Panc-1 (Panc-1-V) and Panc-1-M13 were seeded into 4-well chamber slides and incubated overnight. Cells were treated with 15 µM of SPION-CUR-MUC13 overnight. Cellular uptake of SPION-Anti-MUC13 particles was determined by

Immunofluorescence staining. MUC13 expressing and null Panc1 cells were seeded and treated with different concentrations of SPION-MUC13. After 4hrs, secondary alexafluor-cy3 fluorophore mouse mAb was added and nucleus was stained with DAPI. Subsequently, they were fixed and processed for immunostaining. Slides were examined under a laser confocal microscope (Nikon A1R-HD25 system confocal microscopy).

2.6.3 Internalization of formulation in clinically relevant cell line models, Spheroids

SPION formulation was evaluated for cellular uptake and internalization using 6-coumarin dye in AsPC-1 derived tumor spheroid culture. 6-Coumarin serves as green-fluorescent marker, which was encapsulated with the SPION particles to determine cellular localization and uptake of the nanoparticles. For this, 2 mg 6-coumarin in acetone was added dropwise to 20 mg of SPION particles under stirring condition for 3–4hrs. Cells were seeded in 96 well ultra-low attachment plate and allowed to grow for 7days to form primary spheroids. On 8^{th}day cells were treated with SPION-Coumarin-6 and allowed to form secondary spheroids in ultra-low attachment 6 well plate following immunofluorescence under confocal microscopy. The results obtained show the efficient internalization of curcumin labelled SPION particles. The fluorescence level of the dye tagged particles were confirmed by fluorescence microscopy and images captured at 200X magnification.

2.7 Anti-Cancer Efficacy of SPION-CUR formulation in Pancreatic Cancer cells

Proliferation Assay

Cell proliferation assay was performed to check cytotoxicity of the formulation in Pancreatic cancer cells (Aspc-1, Panc-1, HPAF, and KPC). Cells (0.8×10^6- 0.6×10^6 cells each in 6-well culture plates) were treated with SPION (SP-20 mM), CUR (15 μM), SPION-CUR

(15 μM), SPION-CUR (20 μM) to determine their effect on cell proliferation. SPION highest concentration was used as control. After incubation for 48hrs, changes in cell proliferation were analyzed using cell counting by Invitrogen Cell Countess.

Spheroid Assay

Primary tumor spheroid was developed using KPC cell lines. This assay mimics the tumor microenvironmental condition and we investigated the effect of CUR (2 μM, 5 μM, 10 μM), SPION-CUR (2 μM, 5 μM, 10 μM) as compared to SPION (10 μM control) in spheroid formation ability. KPC cells (3000/well) were seeded in 96-well low attachment plate (Corning) in DMEM/F12 complete media and treated them with previously mentioned treatment groups for 5-7days. After one-week primary spheroids were photographed and compared with the size of SPION (control).

Clonogenicity Assay

Colony formation assay was performed to investigate the effect of SPION-CUR on the colony forming ability of pancreatic cancer cells, as described previously (Khan S et al., 2015). Cells were seeded in 24 well plate with 250 cells per well. Briefly, KPC cells were treated with SPION (control), Cur (2.5 μM and 5 μM), and SPION-CUR (2.5 μM and 5 μM). Colonies were fixed, stained with crystal violet after 7days and photographed. Colonies were counted manually and plotted as a percent clonogenicity. SPION colonies were considered as 100%.

Wound Healing Assay

Cell migration was analyzed using wound healing assay, as described before (Khan et al., 2015). Cells were seeded in 24 well plate with 85,000 cells per well to form a monolayer. Next day cell monolayer was scraped using a 200μL micropipette tip and treated with SPION (control),

Cur (15μM), SPION-CUR (10μM) and SPION-CUR (15μM), SPION-CUR (20μM) in KPC cell line. After 48h of treatment the residual gap length was captured as described earlier (Khan et al., 2015). The plates were photographed for migrated cells using phase contrast microscope at day 0, 48hrs.

Cell Invasion Assay and Migration Assay

Invasion Assay

Cell Invasion assay was performed to investigate the effect of SPION-CUR on the KPC cells using BD Biocoat Matrigel Invasion Chambers (BD Biosciences) (Khan et al., 2015), as per manufacturer's protocol. Cells were seeded in the upper chamber with 40,000 cells in FBS negative and lower chamber with FBS positive media. After 24- and 48-hrs incubation, the invading cells were fixed with methanol and stained with crystal violet. The invaded cells were captured as invasion of the CUR (15 μM), SPION-CUR (10 μM, 15 μM, 20 μM) treated cells compared to control (SPION).

Migration Assay

Cell migration assay was performed to investigate the effect of SPION-CUR on the KPC cells using 96 well insert migration Chambers (BD Biosciences), as per manufacturer's protocol. Cells were starved overnight with FBS negative media and next day counted. 35,000 cells were added to upper chamber along with treatments in FBS negative media. While lower chamber added with FBS positive media. After 12- 18hrs incubation, the migrating cells were fixed with methanol and stained with crystal violet. The migrated cells were captured as migration of the CUR (20 μM), SPION-CUR (10 μM, 15 μM, 20 μM) treated cells compared to control (SPION).

2.8 Molecular analysis of SPION-CUR in Pancreatic Cancer Cells

Immunoblotting Assay

Cell lysate of HPAF-II, Panc-1 and KPC cells were used for checking the expression for the PDL-1 and MUC13. Expression of protein was analyzed by immunoblotting with specific antibodies, anti-PDL-1 and anti-MUC13 mAb and anti-β–actin. Later KPC cell line was opted for the treatment; SPION (control), CUR (20 μM), Gem (150 nM), SPION-CUR (20 μM) + Gem (150 nM). Whole cell lysate was prepared, and Western blotting was performed (Jaggi et al., 2005). Expression of protein was analyzed by immunoblotting with specific antibodies, anti-PDL-1, anti-MUC13 mAb and anti-β–actin.

Real Time PCR

Total RNA was extracted from HPAF, Panc-1 and KPC cell lines using TRIZOL reagent (catalog number AM 9738, Invitrogen). The expression of genes was normalized to the GAPDH gene and fold change for the gene PDL-1 and Muc13 was quantified and plotted on a graph. For studying the PDL-1 gene expression level in CUR/ SPION-CUR (15 μM) treatments, total RNA from KPC cell line was used.

3. RESULTS

3.1 Design and Preparation of SPION-CUR-MUC13 Formulation for Pancreatic Cancer

Pancreatic ductal carcinoma PDAC is rich with complex tumor microenvironment which makes it harder for drug delivery. Our novel nano formulation of SPION-CUR has shown to inhibit this stromal barrier with increased uptake of gemcitabine (Khan et al., 2019). In this proposed study we have conjugated this nano formulation with an in-house generated mucin antibody known

as MUC13 to specifically deliver the therapeutics to the tumor sites. Clinical and pathological analysis of PDAC has shown aberrant expression of MUC13 glycoprotein (Khan et al., 2018), which makes MUC13 an ideal targeting marker. Our SPION-CUR has the ability to direct towards the pancreatic tumor core and can release the drug more efficiently.

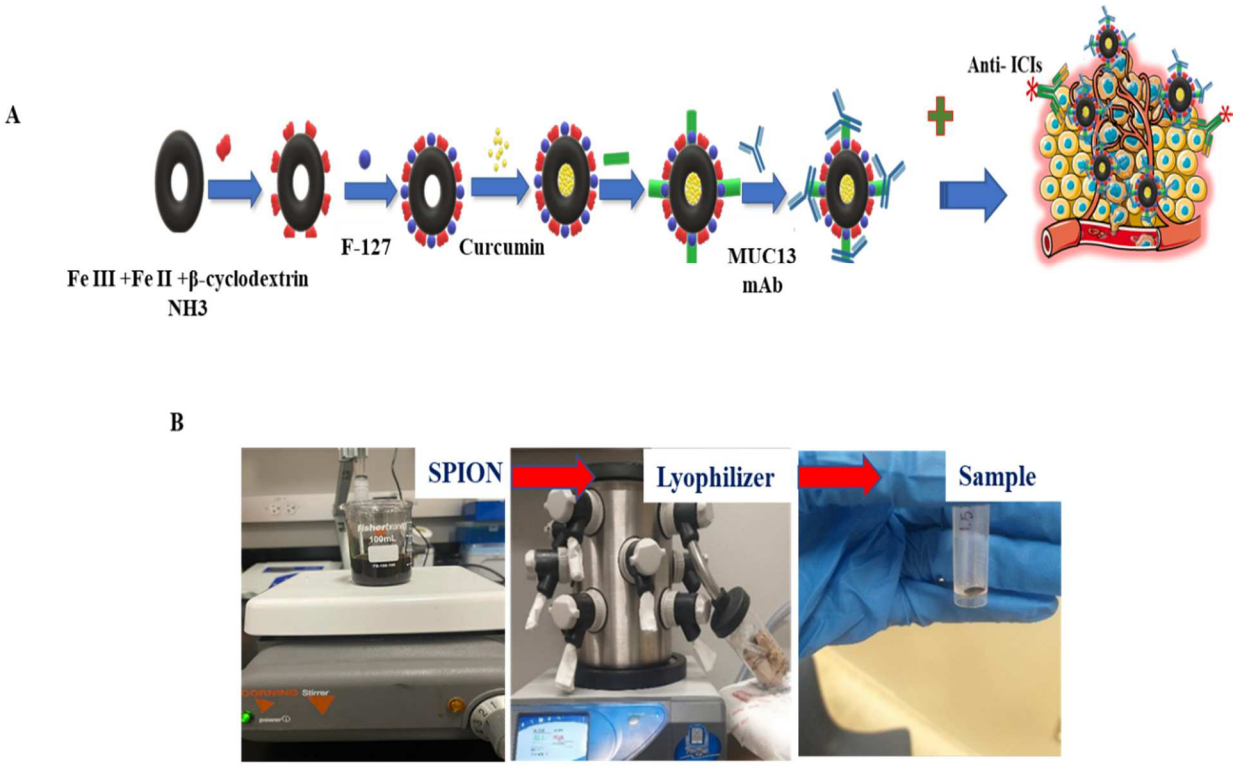

Fig. 4. Generation of SPION-CUR-MUC13mAb nano formulation (A) Schematic representation demonstrating generation of SPION-CUR-MUC13 and its targeting ability towards the tumor microenvironment. At first, iron core of SPION was stabilized with polymers β-cyclodextrin and F-127 and then loaded with curcumin. Muc13mab was later conjugated with the help of NHS linker (B) Lyophilization of SPION nano formulation to determine the weight of the stabilized iron core.

The SPION-CUR was successfully formulated and stabilized with polymers β-cyclodextrin and F-127 as depicted in the Fig. 4 (A) and later conjugated with in-house generated MUC13mAb for targeting pancreatic tumor with the help of NHS-linker. Additionally, we lyophilized the formulation using a lyophilizer machine to determine the core weight Fig. 4 (B) Average of 7- 10 mg/ml was obtained every time and this formulation could be stored at 4□ for 1 week (Table.1). New batches were made every time prior to each treatment. Weight of the iron core was determined using empty tube method, where weight of the tube with and without lyophilized nano formulation was calculated. SPION-CUR carries 10part of SPION and 1part of curcumin (10:1). That means for every 10mg of SPION we have added 1mg of curcumin making a stock concentration of ~2 mM.

3.2 Characterization of the SPION and SPION-CUR formulations reveals efficient Particle Size and Zeta Potential

Successful delivery of SPION-CUR depends on its size and charge. Size and charge of the SPION before and after loading curcumin was determined with the Zetasizer machine. Size of the nano formulation was determined by dissolving 150 µl of nano formulation in 3 ml of distilled water and ran for 3 repeats and average was calculated. Our formulation has demonstrated an optimum average size range of 96.76 nm for SPION and 115.9 nm for SPION-CUR (M. M. Yallapu et al., 2013). Charge of the formulation was determined by dissolving 50µl nano formulation in 1ml of 1X PBS, preferable negative charge was obtained for both SPION and SPION-CUR. The average zeta potential of the formation was -25.8 mV for SPION and -21.39 mV for SPION-CUR (Table. 2) (Fig. 5).

A

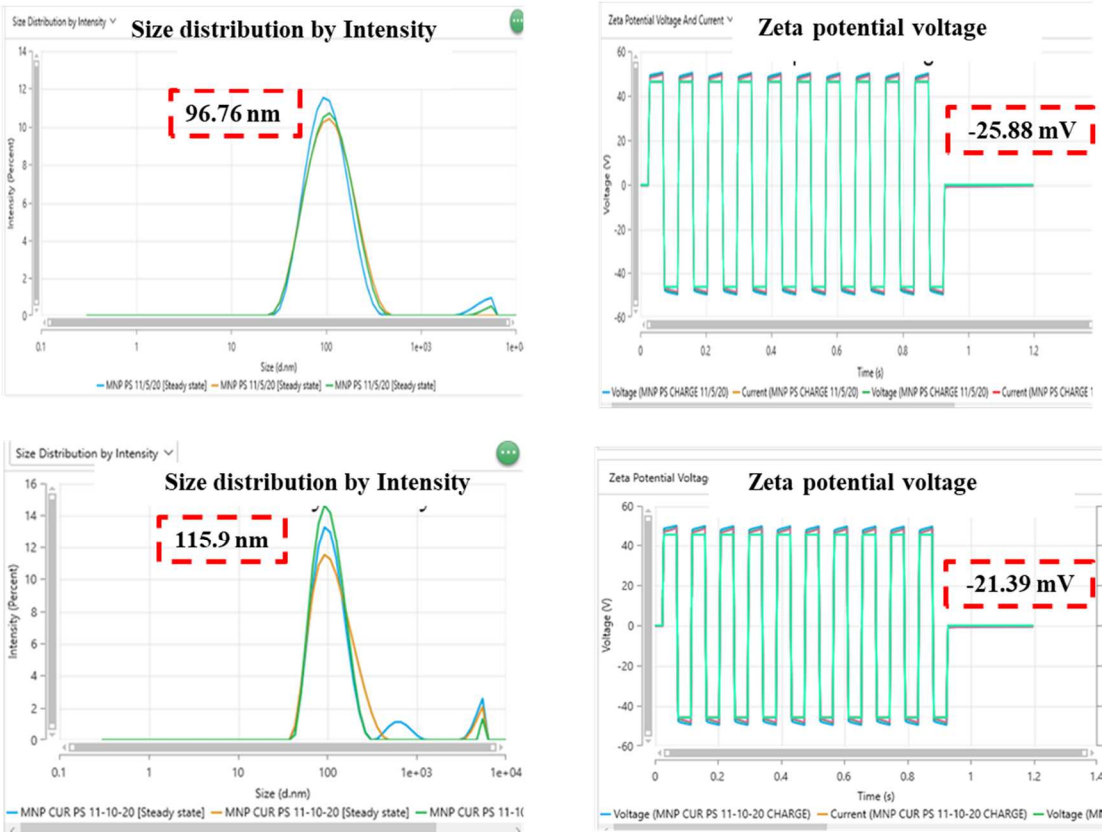

Fig.5. Characterization of SPION-CUR-MUC13 nano formulation, graphs illustrating the size and charge distribution of (A) SPION and (B) SPION-CUR nano formulation using Zetasizer. Size distribution by intensity was measure in nanometer scale and zeta potential of the formulation was measured in voltage.

3.3 Nanoparticle Formulation internalizes Efficiently in Pancreatic Cancer Cells

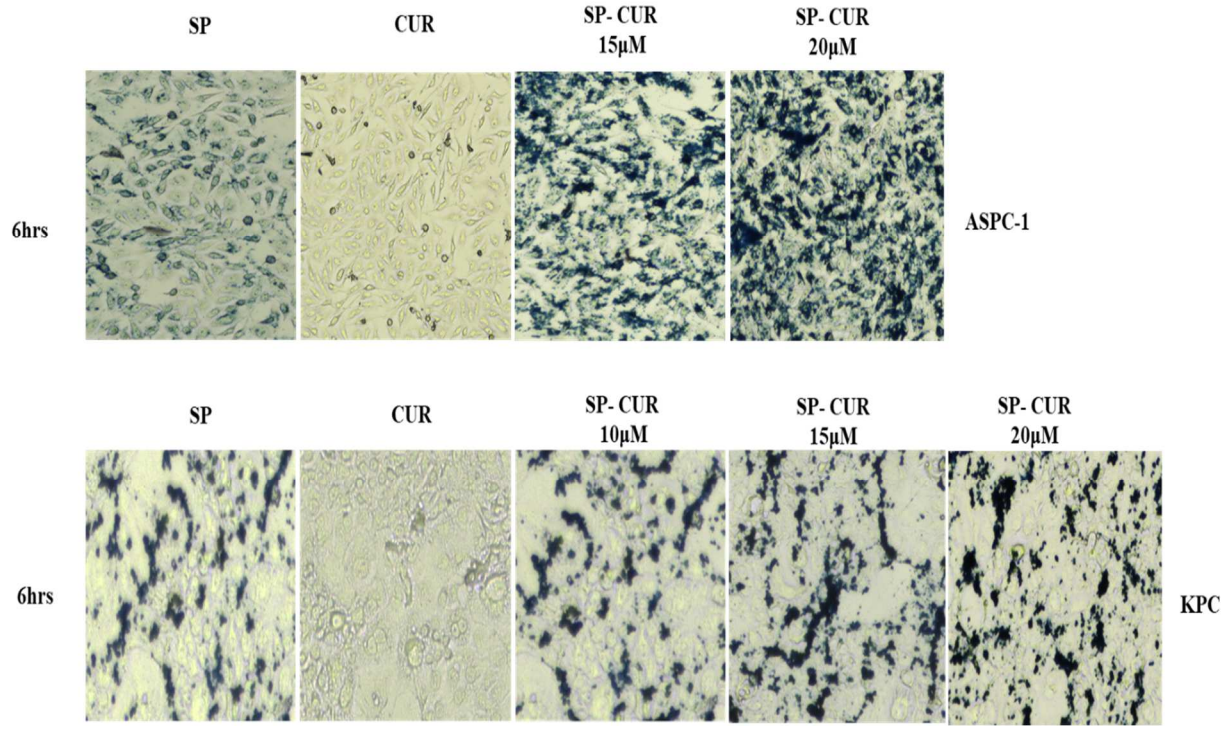

Fig. 6. Internalization of SPION-CUR nano formulation using Prussian blue staining. Prussian staining was performed to determine the cell uptake efficacy of SPION(SP), CUR and SPION-CUR (SP-CUR) in (A) ASPC-1 and (B) KPC cell lines after 6hrs of incubation.

Prussian staining is one of the methods used to determine the cellular uptake of iron particles. This staining technique determines whether the cell has iron content, then it reacts and generates a blue color as an indicator. SP-CUR dyed with Prussian blue were detected as dark blue spots formed by ferric to ferrous iron reduction. At 6hrs, the data clearly demonstrate the presence of nanoparticles within the cells, with a dose-dependent intake of the SP-CUR formulation.

Nanoparticle uptake was consistent in pancreatic cancer cells, indicating that these particles are flexible and can deliver treatments effectively.

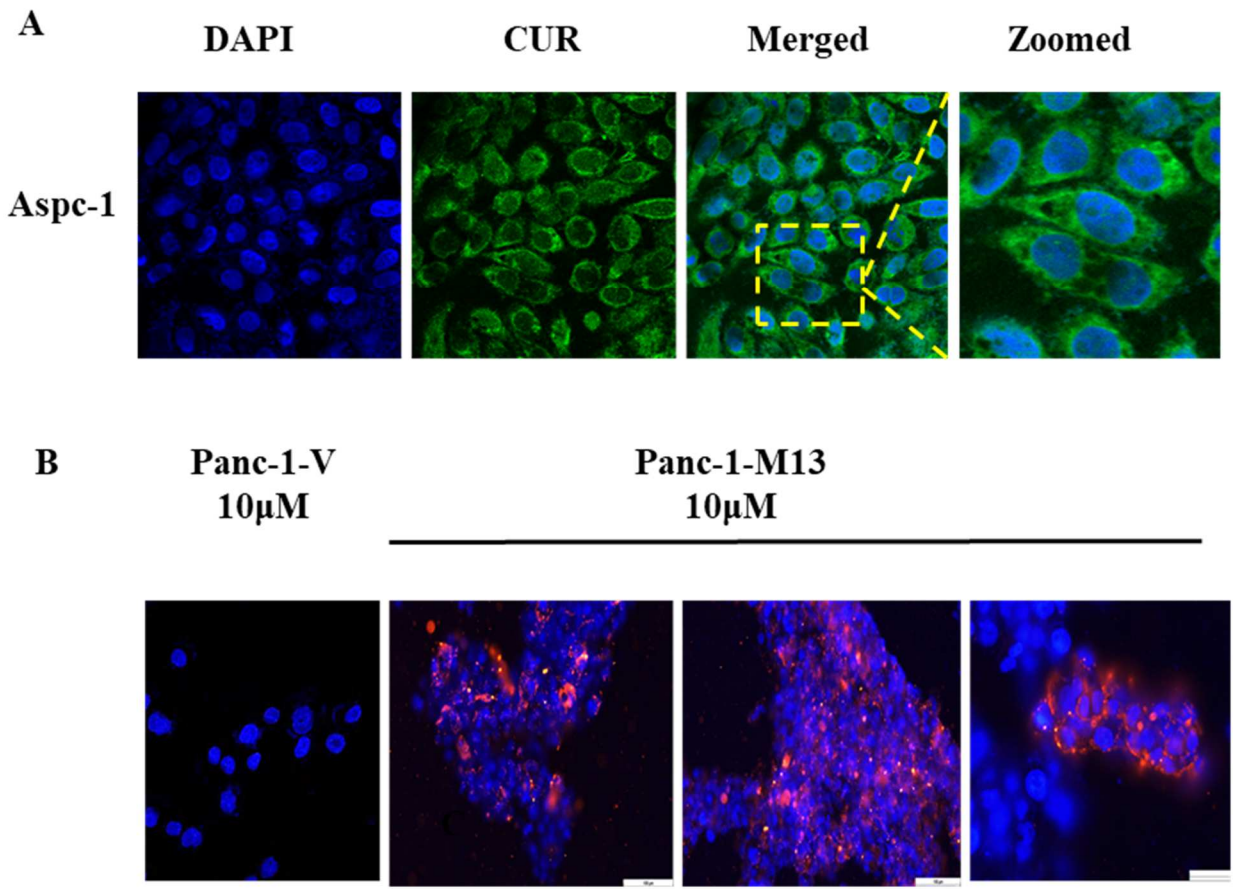

Fig. 7. Internalization of SPION-CUR and SPION-MUC13 nano formulation using Immunofluorescence in (A) AsPC-1, Curcumin (green), DAPI (blue) and (B) MUC13 null and positive cells, (Panc-1-V and Panc-1-M13), the color red represents MUC13, and blue is the nuclear staining using DAPI.

We also performed confocal immunofluorescence to investigate the ability of formulation to internalize efficiently into the cells. Curcumin has an autofluorescence of green color which can be visualized in immunofluorescence assay. Fig.7A illustrates the effective internalization of

SPION-CUR in Aspc-1 cells as depicted by green fluorescence emitted by the SPION-CUR upon cell internalization. Further, cellular uptake of SPION-MUC13 (SP-M13) particles was determined using Panc-1-V (MUC13 null) and Panc-1-M13 (stably expressing MUC13 positive cell lines). After 18hrs of treatment in cells with SP-CUR-M13, the formulation was observed to efficiently target and internalize MUC13 expressing Panc-1-M13 cells as compared with Panc-1-V cells, which do not express MUC13. This is depicted by fluorescence (red) in the images by using confocal microscopy (Fig. 7B). Alexafluor-cy3 fluorophore mouse mAb was used as secondary antibody and nucleus was stained with DAPI. Images were captured for DAPI (blue) and MUC13 (red) in pancreatic cancer cells. Therefore, these results suggest that the SP-CUR-M13 efficiently targets MUC13 in Panc-1-M13 cell line, which stably expresses MUC13 (Fig. 7 B).

Cellular uptake of SPION-Anti- MUC13 particles was determined by confocal immunofluorescence staining using KPC cell line (Fig. 8). After 4 hours of treatment with SPION-MUC13, the immunofluorescence staining detected SPION-MUC13 internalization in KPC cells, which increased upon increased treatment dose. The uptake of formulation increased directly with increase in the concentration as depicted by higher red fluorescence at 30μM. The fluorescence was captured by the secondary antibody, alexafluor-cy3 fluorophore mouse mAb (red) and a nuclear stain was performed using DAPI. This experiment was performed to determine the internalization of MUC13 in KPC cell lines that express MUC13. While SPION without MUC13 conjugation showed no red color. (Fig.8).

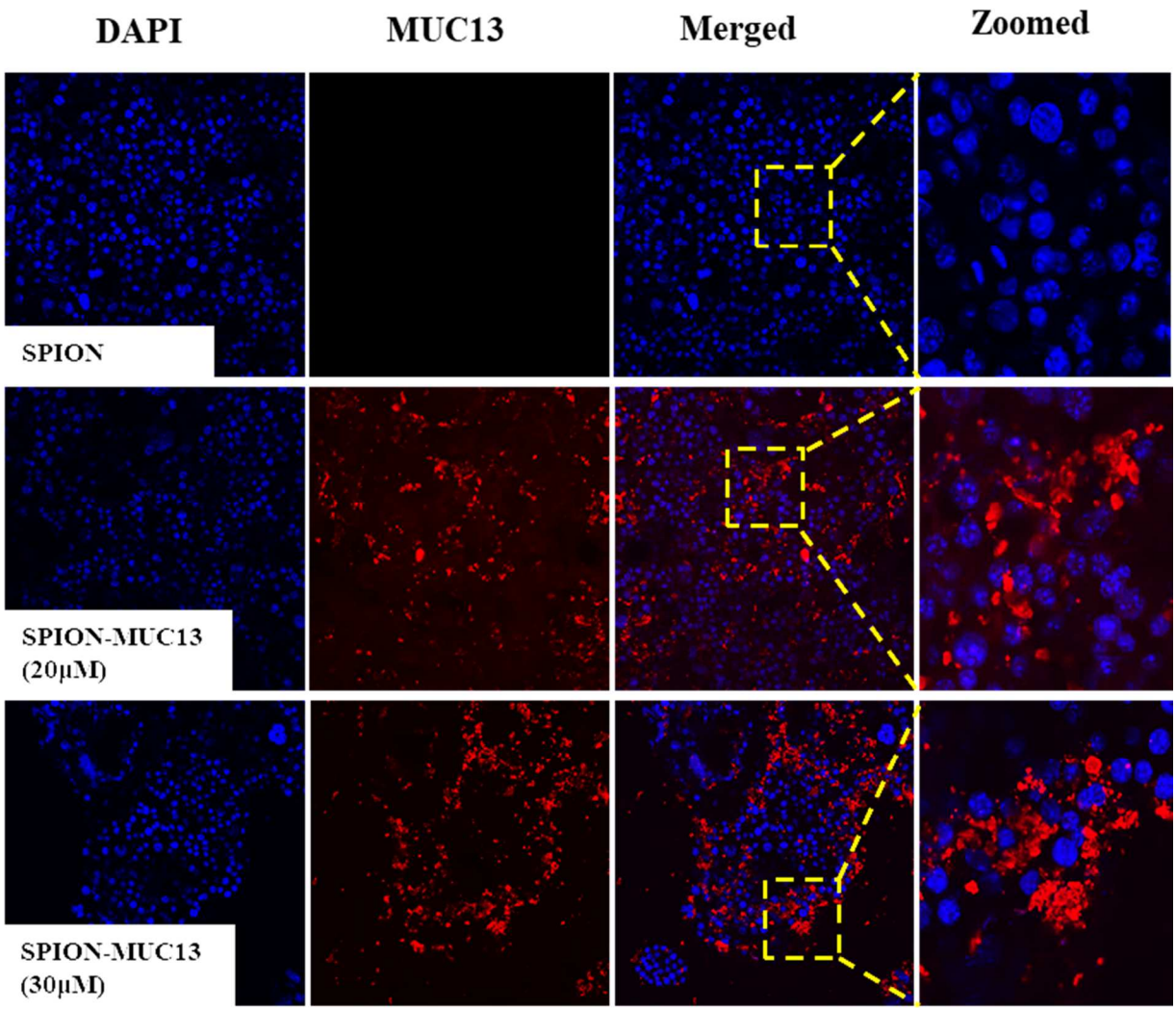

Fig. 8. Internalization of SPION and SPION-CUR-MUC13 nano formulation using confocal Immunofluorescence in KPC cell lines. SPION-CUR-MUC13 cell uptake was investigated with different concentrations of SPION-CUR-MUC13 formulation in mouse cell line.

Coumarin Staining in Spheroids

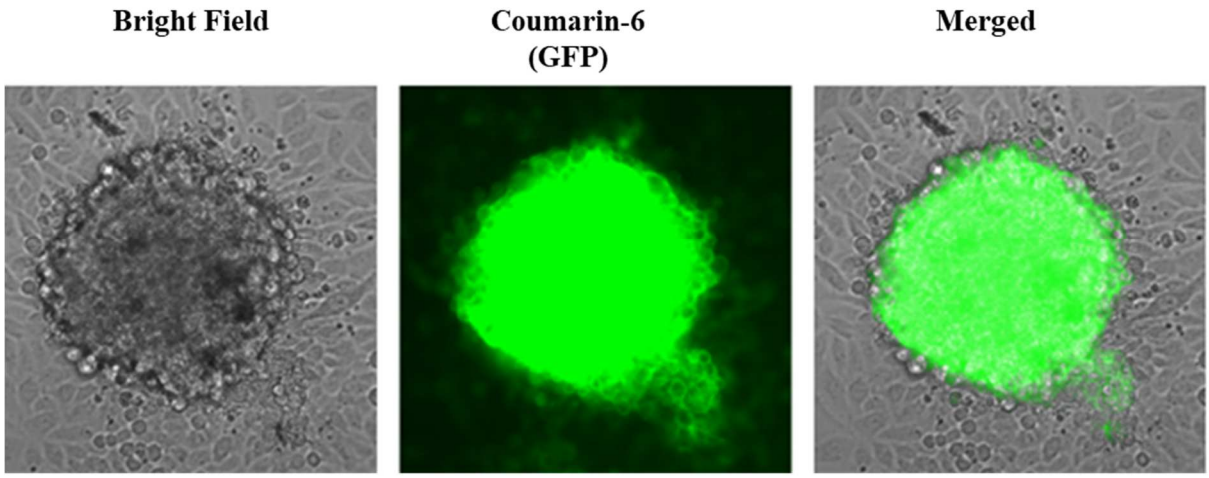

Fig. 9. Internalization of SPION nano formulation using coumarin-6 dye in secondary Aspc-1 spheroids. Image illustrated the internalization of SPION into the spheroids (green).

Spheroids serve as an *in vitro* three-dimensional multicellular model that can mimic a solid tumor. To understand the clinical relevance of our formulation, we have generated spheroids and stained with coumarin dye which can detect the presence of Iron content. We observed efficient internalization of the formulation into the spheroids as depicted by the green fluorescence associated with coumarin conjugated SPION formulation using microscopy (Fig. 9). These results suggest the clinical relevance of our studies and that the SPION nano formulation can efficiently penetrate the tumors.

3.4 SPION-CUR formulation inhibits proliferation and cell viability in pancreatic cancer cells

Cell proliferation Assay

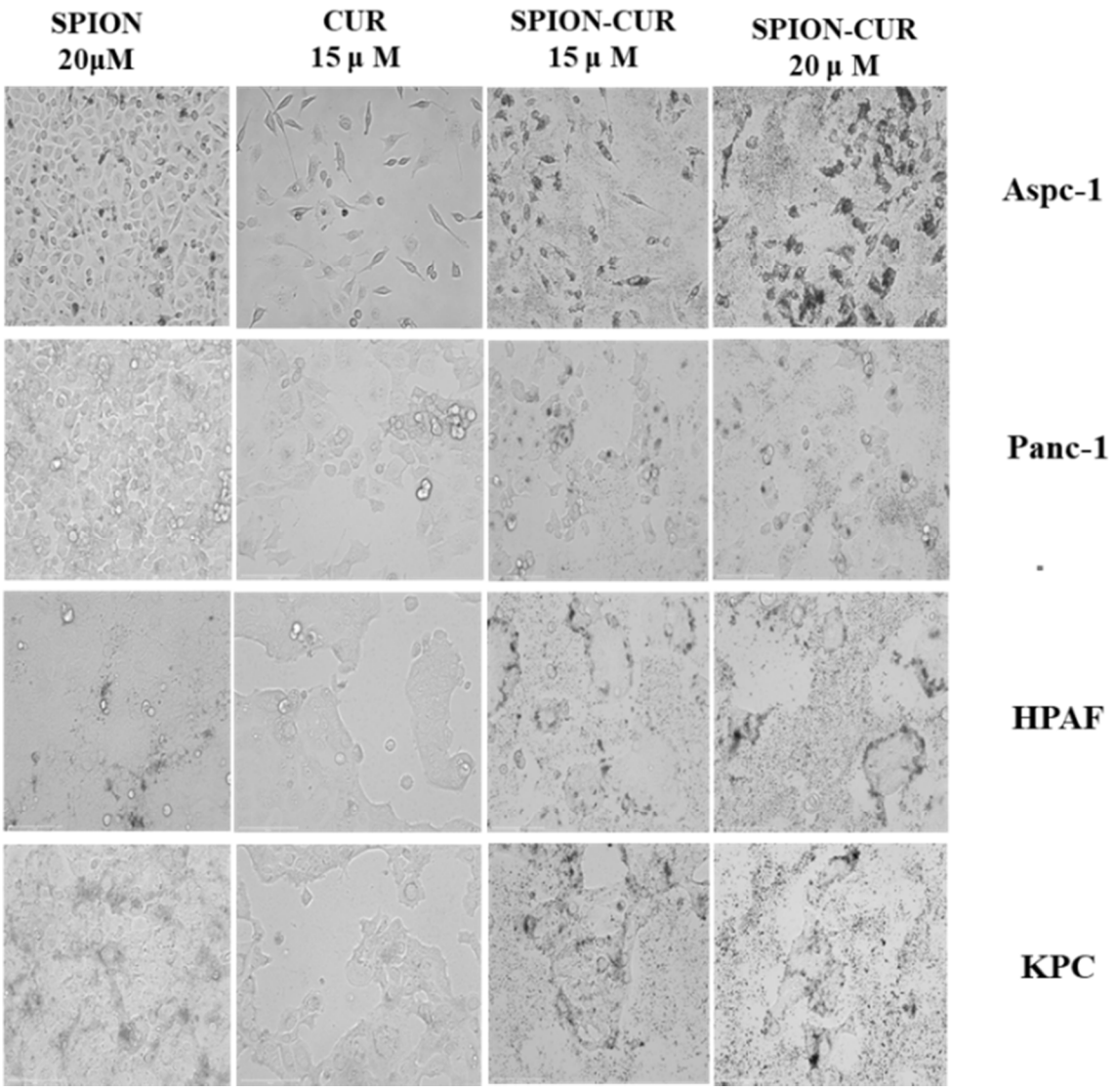

Fig. 10. Proliferation assay to investigate the effect of SPION-CUR nano formulation on proliferation of cells, Aspc-1, Panc-1, HPAF, and KPC cell lines. SPION-CUR with different concentrations was treated and compared with curcumin and SPION (control).

Curcumin is known to have anti-cancer and anti-inflammatory activities. We investigated the effect of SPION-CUR on proliferation and morphology of cells upon treatment in different cell lines such as Aspc-1, Panc-1, HPAF, and KPC. SP-CUR demonstrated inhibition of cell proliferation with an increase in treatment as compared to the SPION (Control) and curcumin. Curcumin alone has shown some anti-proliferative effect, but this effect was comparatively less when compared with higher concentration (Fig.10). SPION-CUR exhibited a dose-dependent inhibition of cell proliferation.

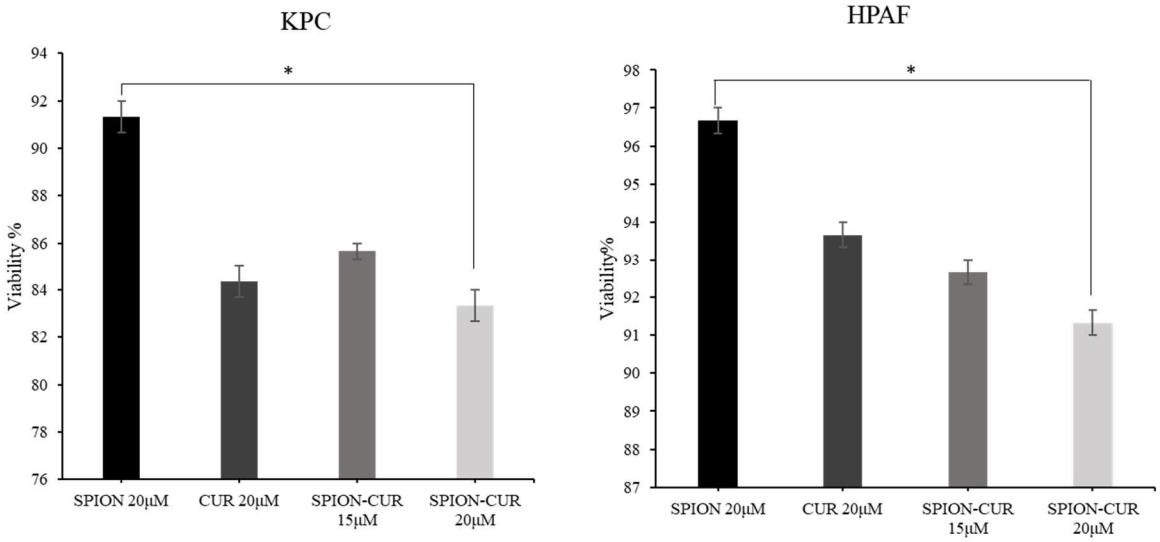

Fig. 11. Cell viability assay was performed in KPC and HPAF pancreatic cell lines. Cells were treated with different concentrations of the formulation. The bar graphs are plotted against average values for the treatment effect. P value is less than 0.005, this difference is considered to be extremely statistically significant.

Cell viability assay was performed in HPAF-II and KPC cells to determine the percentage of live cells upon treatment with various concentrations of our formulation. After 48hrs of incubation, live cells were counted from each group using automated cell counter (Invitrogen Cell Countess) and percentage of viability obtained from counting was used for

plotting graph. In both HPAF and KPC cell lines, percentage viability decreased upon treatment with formulations.

SP-CUR formulation demonstrates clinical significance in pancreatic cancer

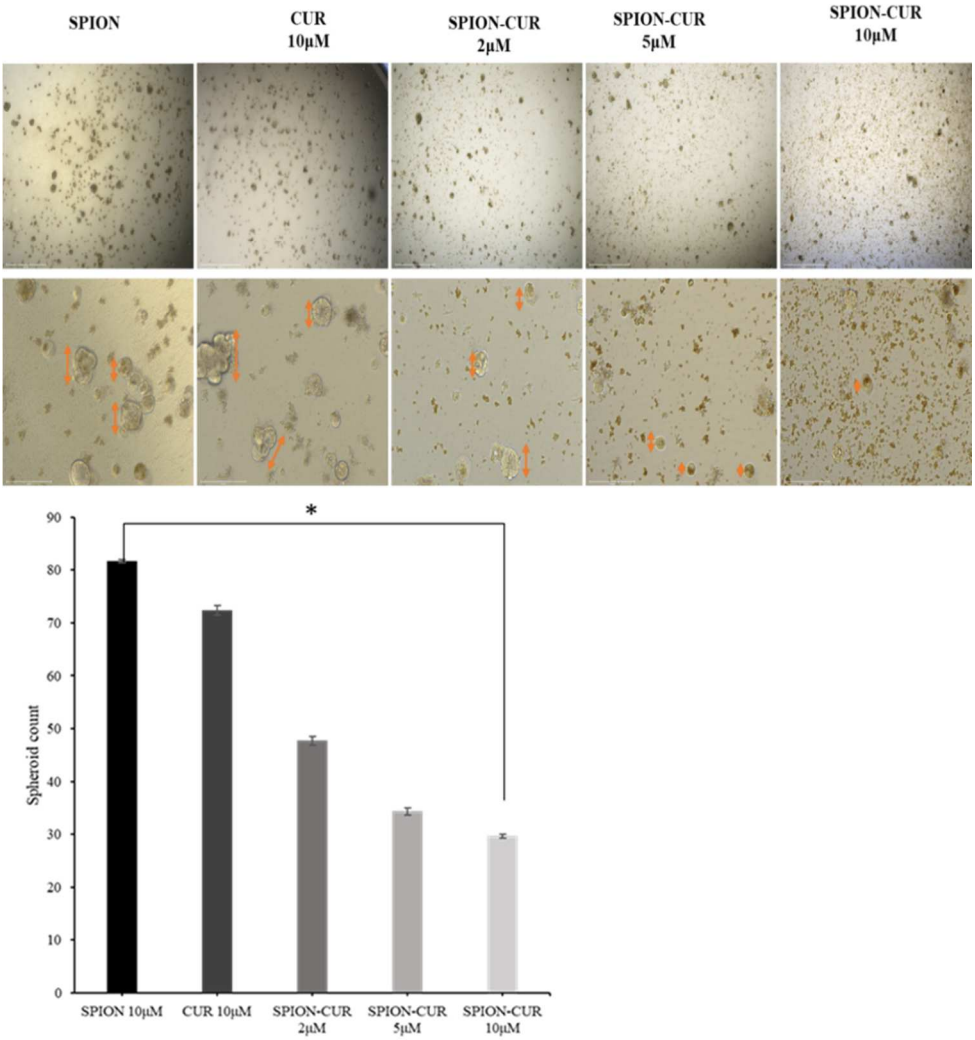

Fig. 12. Spheroid assay, KPC primary spheroids were treated with SPION-CUR, CUR and SPION (control), analyzed, counted, and captured at 4X and 10X. The graph illustrates number of spheroids from each treatment group. P value is less than 0.005, by conventional criteria, this difference is considered to be extremely statistically significant.

Primary spheroids mimic the tumor and serves a good *in*-vitro 3D model to check the anti-cancerous effect of SPION-CUR. The ability of the formulation to inhibit primary spheroid formation was investigated. The number of spheroids formed in presence of treatment was analyzed and counted for each treatment groups (Fig. 12). The results showed decrease in number of spheroids as well as in size with the increase in treatment concentrations of SPION-CUR. These observations further depict that the development of primary tumor spheroids was restricted with SPION-CUR treatments when compared to CUR and SPION (control).

SP-CUR inhibits the Invasion, Migration and Clonogenicity of KPC cells

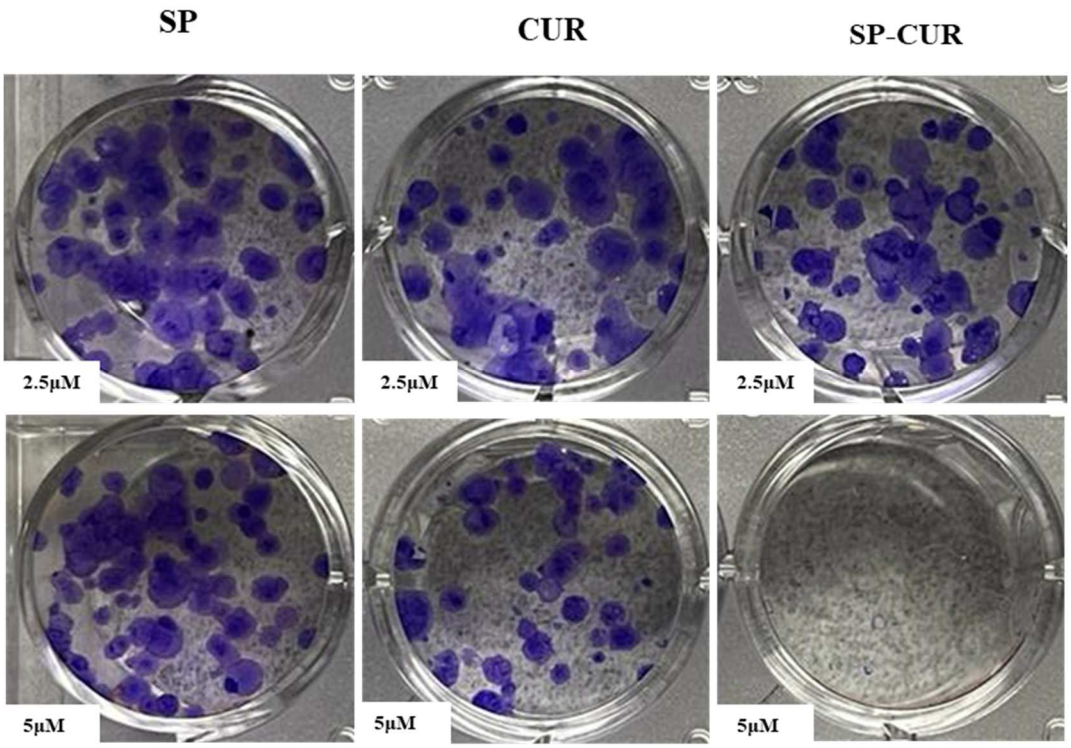

Fig. 13. Therapeutic efficacy study of SPION-CUR using clonogenicity assay. The effect of SPION-CUR on colony formation ability was studied in KPC cell line. Colonies of KPC was generated and treated with treatment groups, crystal violet staining was performed to visualize the colonies.

Colony formation ability is one of the hallmark of cancerous cell as it helps the cell to expand and migrate to distant areas or even organs. Our result demonstrates that the size and number of colonies were largely restrained with SPION-CUR when compared to curcumin and SPION (control). Higher concentration of SPION-CUR inhibited the colonogenic ability of the cells and yeilded no or less colonies (Fig. 13). SPON-CUR exhibited a dose-dependent inhibition of colony formation.

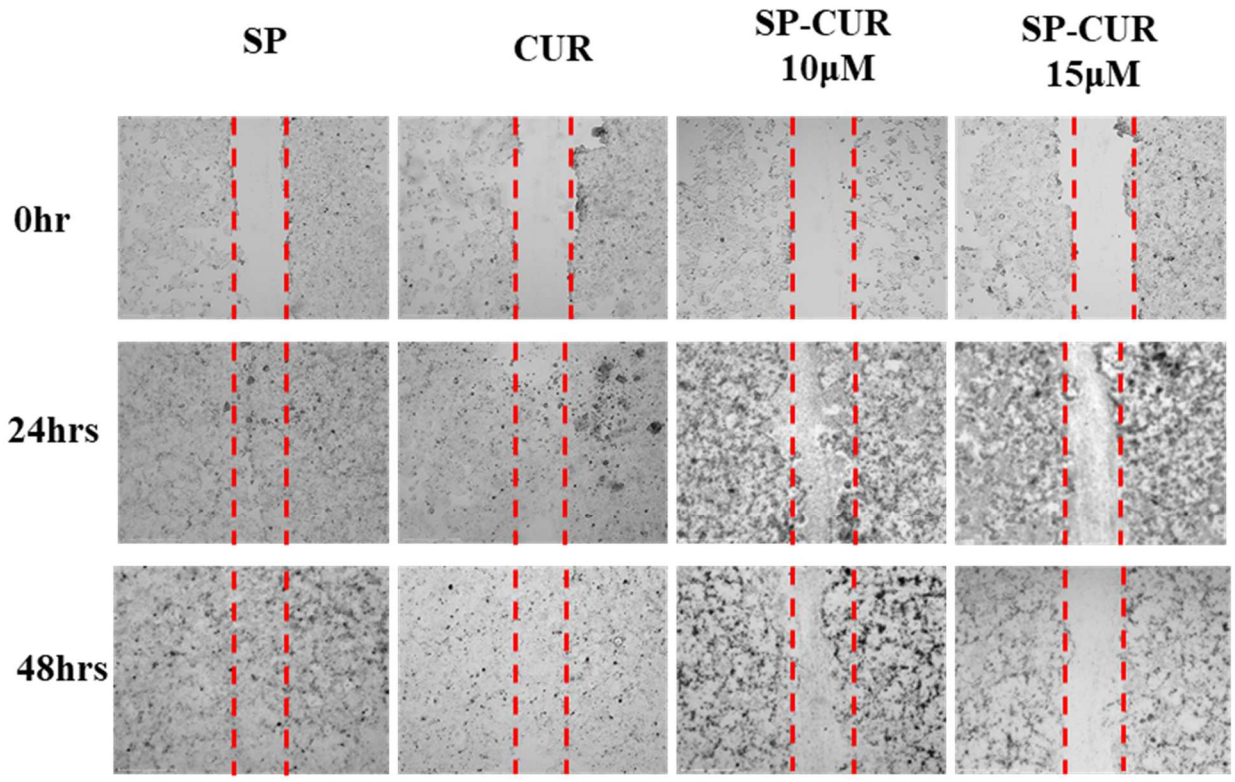

Fig. 14. Therapeutic efficacy study of SPION-CUR using wound healing assay. Wound healing was performed to determine the healing ability of KPC cells after a wound formation. KPC cells were treated for 48hrs, image was captured at 0hr, 24hrs and 48hrs.

Wound healing assay is a molecular technique that utilizes a creating of a wound in the cells to investigate the migratory ability of cells that can lead to wound closure. As depicted in Fig. 14, the cell migration ability of KPC was observed to be inhibited upon SPION-CUR treatment. The initial (0hr) and the residual gap length at 48hrs after wounding, were analyzed and captured. Cells were washed with 1X PBS every time before capturing the images. The treatment with higher concentration of SPION-CUR remained to have same residual gap length, whereas SPION (control) and curcumin alone completely or partially closed after 48hrs (Fig. 14).

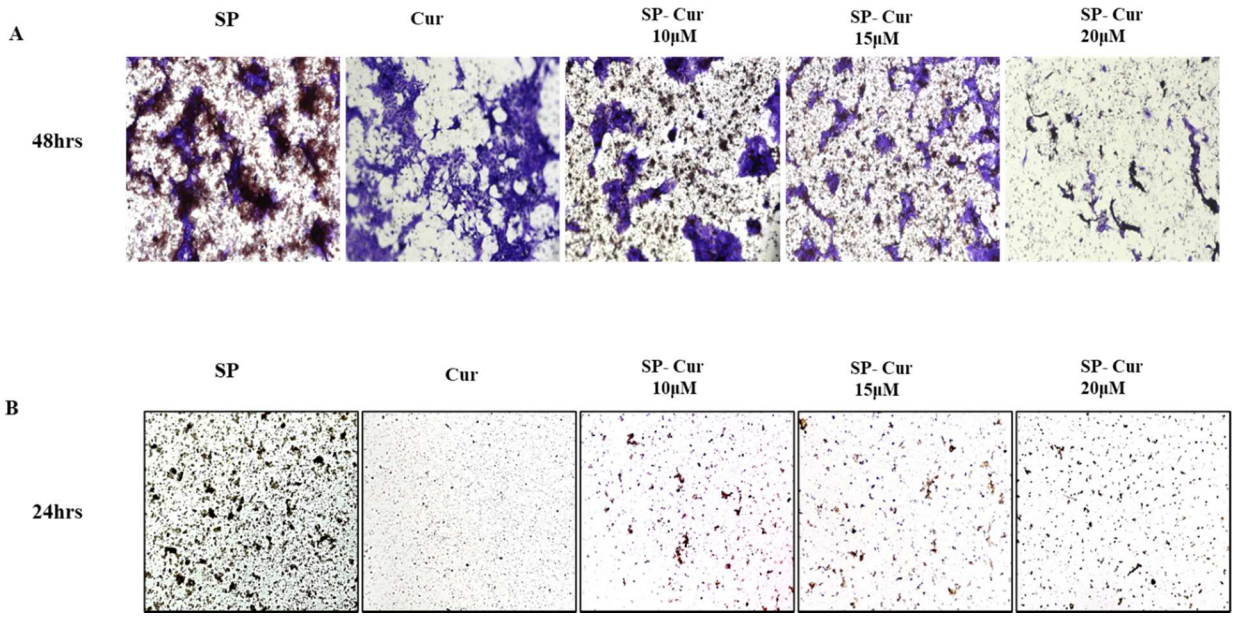

Fig. 15. Therapeutic efficacy study of SPION-CUR using (A) Invasion assay and (B) Migration assay in KPC cell line. The crystal violet staining the blue color depicts the cell invasion and the hematoxylin staining the red color depicts cell migratory ability of KPC after treatment.

Pancreatic cancer cell invasiveness and migration of KPC cells were analyzed and images captured. Cancer cell has the ability to invade and migrate towards the media containing FBS, which is known as chemotaxis. After the treatment, the ability of KPC cell lines to invade was decreased with increased concentration of SPION-CUR (10, 15, and 20 μM). SPION-CUR decreased the number of invading cells with higher concentration, clearly suggesting that SPION-CUR inhibit KPC cell invasion (Fig 15 A). Similar results were found in migration assay that showed SPION-CUR decreased the number of migratory cells with the increase in concentration (Fig. 15 B).

3.5 PDL-1 and MUC13 is expressed in KPC cells and SP-CUR does not affect PDL-1 expression

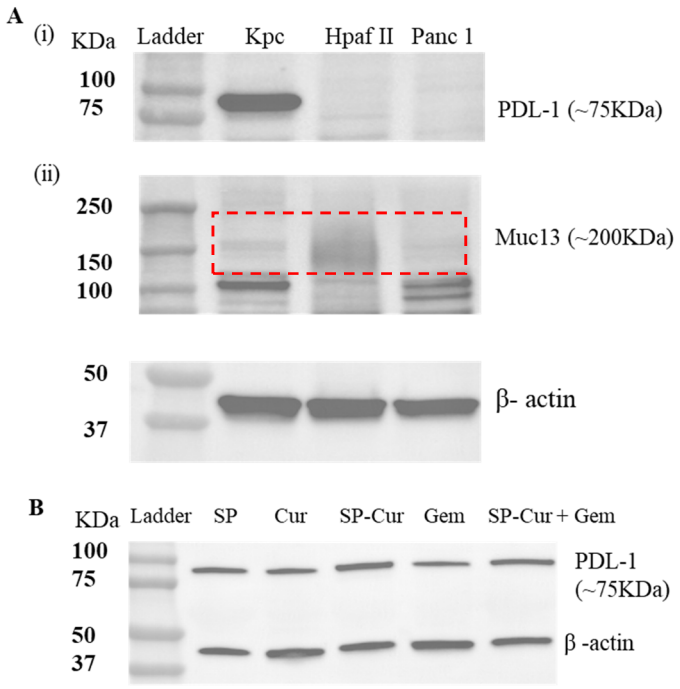

Fig. 16. Immunoblotting Assay was performed in (A) KPC, HPAF, and Panc-1 cell lines to study the expression level of proteins (i) PDL-1 and (ii) MUC13, with β-actin as the control. (B) KPC cell line to study the expression level of PDL-1 (ICI) after treatment.

Our study aims at targeting the MUC13 tumor microenvironment and strengthening the immune checkpoint inhibitor therapy. For this, we have used three different cell lines KPC, HPAF and Panc-1 to check expression of MUC13 and PDL-1 (Fig. 16 A). The expression of PDL-1 demonstrated the upregulation of PDL-1 protein in KPC cell line when compared with HPAF and Panc-1(Fig.16 A(i)). Similarly, expression of MUC13 protein was studied in three different cell lines, MUC13 expression was highly upregulated in HPAF, moderate in KPC and downregulated Panc-1 (Fig.16 A(ii)).

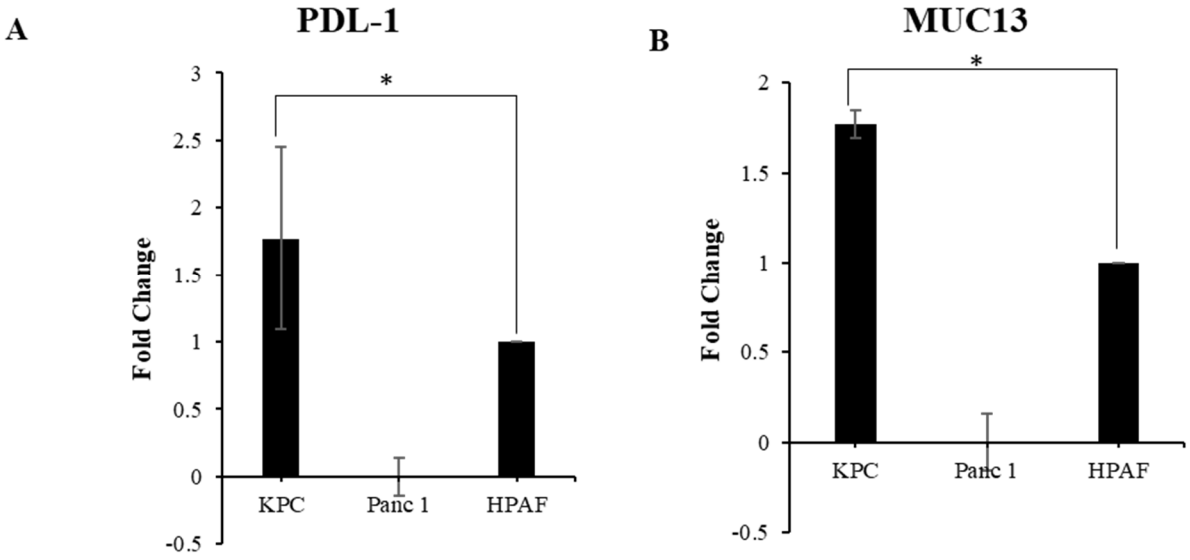

Fig. 17. Real time PCR. Expression study was performed in three different cell lines, KPC, Panc-1, HPAF for (A) PDL-1 (B) Muc13. (B) Expression study of PDL-1 (ICI) gene was studied in KPC cells for the treatment groups. ($P < 0.0005$)

Our lab has studied therapeutic effect of SPION-CUR upon treatment with gemcitabine in HPAF and Panc-1, but not in KPC (Khan et al., 2019). Additionally, we sought to investigate if

SP-CUR treatment alters the expression of PDL-1 in KPC cells. No significant changes in the expression of PDL1 was observed on protein levels, which warrants combination studies of SP-CUR with anti-PDL-1 checkpoint therapy (Fig.16 B). Overall, our result on KPC cell line supports the previous data that SPION-CUR inhibits pancreatic cancer cells. For further therapeutic analysis of SPION-CUR, KPC cell line was used for both in *vitro* and *in vivo*. Similar results were corroborated with real time PCR, demonstrating KPC cells having both MUC13 and PDL-1 protein expression. KPC cell line has shown significantly higher fold change of PDL-1 (<0.005) and MUC13 (<0.0005) when compared to HPAF and Panc-1 (Fig 17 A & B).

4. DISCUSSION

Pancreatic cancer (PanCa) is a third leading cause of cancer related deaths in US due to late diagnosis and development of chemo-resistance. Chemoresistance and ineffectiveness of therapeutics in pancreatic cancer regimen are attributed to aggressive, fibrotic pancreatic tumor microenvironment, which makes pancreatic tumors very hard to tackle. Many stroma targeting drugs have adverse side effects so are not feasible to be used. Therefore, alternate delivery mechanisms are required to hit the grounds and deliver the therapeutic efficiently to the tumor area. For this, a combination of a drug that inhibits stroma and better tumor targeting modality is necessitated. Mucin, MUC13 is aberrantly expressed in PanCa, promoting cancer growth and progression. Unlike other cancer types, PanCa is highly resistant to chemo drugs due desmoplasia and fibrotic tumor microenvironment (TME) that makes it very important to find alternate treatment strategies for efficient delivery of therapeutics that are targeted specifically to the tumor site. Herein, we demonstrate the integration of novel approach to specifically target and deliver therapeutics to the pancreas tumor site. For this, we have used a rational combination

our recently generated SPION-CUR nanoparticles and our in-house generated MUC13 monoclonal antibody that has the ability to target the tumor site and deliver therapeutics. SPION-CUR nanoparticles are utilized to overcome stromal barrier and MUC13 antibody conjugation is utilized for tumor specific delivery. Therefore, this chapter III describes the generation, characterization and functional efficacy of this therapy in *in vitro* cell line models, including KPC cells that have been generated from very fast growing KPC mouse model (Pdx1cre;LSL-KrasG12D;LSL-Trp53R172H) mice. KPC cells are clinically relevant *in vitro* cell line models as the mice recapitulates the disease progression seen in humans.

Herein, we demonstrate cellular delivery, uptake/internalization capability of SPION-CUR/ SPION-CUR-MUC13 (Fig. 6&9) and potent anti-cancer effects of this novel SPION-CUR formulation in pancreatic cancer cell line models, including KPC cells. Successful delivery of SPION-CUR and SPION-CUR-MUC13 was investigated by immunofluorescence assay (Fig. 7&8). This delivery system has been used in the previous studies from our lab to deliver anti-cancer drugs (Khan et al., 2015; Khan et al., 2019; M. M. Yallapu et al., 2013; Murali M Yallapu et al., 2012). In the present studies, we have utilized this delivery mechanism for developing tumor specific targeted therapeutic delivery system to pancreatic cancer site using MUC13 antibody conjugation.

MUC13-SPION formulation led to an enhanced uptake in MUC13 positive ($MUC13^{+ve}$) PanCa cells as compared with MUC13 null ($MUC13^{-ve}$) cells as demonstrated by immunofluorescence, Prussian blue staining and flow cytometry experiments. Interestingly, the formulation resulted in sustained delivery of CUR, enhanced inhibition of cell proliferation, migration and invasion in $MUC13^{+ve}$ cells as compared with $MUC13^{-ve}$ cells, which suggests the targeting efficacy of the formulation. Additionally, the treatment of cells with the formulation

inhibited the tumor spheroid formation and growth. Spheroid assay results shown increased therapeutic application of SPION-CUR on primary spheroids by reducing the spheroid formation ability in KPC cell lines (Fig. 12). The primary advantage of spheroids is that it can mimic hypoxia nature of tumor. Further we checked the effect of SPION-CUR on its ability on colony formation, wound healing, invasion, and migration in KPC cell lines (Fig.13,14 & 15). All the mentioned assays supported the better curcumin intake and anti-cancerous effect of SPION-CUR when compared to curcumin alone. Our results suggest it to be a promising delivery system that could inhibit desmoplasia and target tumor microenvironment with the help of conjugated MUC13mAb. We have previously shown therapeutic application of SPION-CUR in pancreatic cancer cells and in an orthotopic xenograft tumor model of pancreatic cancer (Khan et al., 2019). A strong reduction in cell proliferation and enhanced uptake and sensitivity of cancer cells to GEM upon treatment with SPION-CUR was observed (Fig. 16 & 17). The formulation softens up the tumors for therapies that can result in improved response to checkpoint immunotherapies, which are otherwise ineffective against pancreatic tumors.

5. CONCLUSION

Results indicate high therapeutic significance of MUC13-SPION for achieving targeted pancreatic tumor specific delivery of therapeutics. Since SPION-CUR particles inhibit the fibrotic immune tumor microenvironment, therefore, MUC13 conjugated SPION-curcumin has a potential to investigate checkpoint immunotherapies, inhibit tumor growth and its progression (NEXT CHAPTER IV). This study has a potential to reduce morbidity and mortality caused by the disease and improve survival in patients.

CHAPTER IV

INVIVO AND *EXVIVO* STUDIES USING SPION NANOFORMULATION FOR PANCREATIC CANCER THERAPY

1. BACKGROUND

Cancer of pancreas remains to be the third most lethal cancer in United States. Only 10% of individuals diagnosed survive 5 years, and there are only few effective treatments available. Immunotherapeutic is a rapidly increasing field of research in cancer biology, but there has been little progress in using it to treat pancreatic cancer. Immune checkpoint inhibition has shown long-term therapeutic responses in a variety of human cancers, but not in pancreatic cancer patients. Attempts to understand this resistance mechanisms and improve the efficacy of immune checkpoint blockade in pancreatic cancer necessitate the use of appropriate preclinical models in the laboratory (Pham et al., 2021). Immune checkpoint antibodies against PD-1, PDL-1 and CTLA-4 are in clinical trials for PDAC treatment, but these treatments have limited success rate due to complex PDAC tumor microenvironment. PDAC's immunosuppressive tumor microenvironment (TME) also contributes to its low immunogenicity. PDAC is characterized by a dense desmoplasia created by pancreatic stellate cells (PSCs). PDAC's stroma is a hypovascular and hypoxic environment, which creates a barrier for infiltrating effector T cells and therapeutic drugs (Zhou et al., 2020). Therefore, associations between cancer cells and the stroma are important for our understanding of cancer growth and progression. Therapies focusing on stromal modulation may have more success in increasing the efficacy of immune checkpoint therapies (Kota, Hancock, Kwon, & Korc, 2017).

The present study is focused on improving immune checkpoint therapies by modulation of stroma. However, relatively few studies have investigated the potential of stroma inhibitors in promotion of immune response because of the side effects associated with available stroma antagonists. In this study, we have used a natural plant agent, curcumin as an effort to potentiate immune checkpoint therapies based on our previous studies displaying its stroma depleting ability (Khan et al., 2019). Curcumin displaying a poor bioavailability remains a major hindrance in its clinical translation. Therefore, our lab has generated a novel patented nanoparticle formulation (SPION) for its efficient delivery to tumor. In this study, we have formulated these SPIONs with MUC13 antibody that can specifically target pancreatic tumors, which aberrantly express MUC13 (SP-CUR-MUC13). This Chapter demonstrates results of combination therapy from our preclinical trial using $Kras^{G12D}$; $LSL\text{-}Trp53^{R172H}$ syngeneic mouse model of PDAC. This trial is conducted to test the efficiency of SP-CUR-MUC13 in improving immune checkpoint therapies (CTLA4 and PDL-4) by targeting tumor desmoplasia and depleting tumor stroma. Our result suggests the possibility of achieving T-cell infiltration into the tumor nest and strengthen the benefits of tumor immune activation by administering Immune checkpoint therapies with SP-CUR-MUC13 that inhibit stromal reactions.

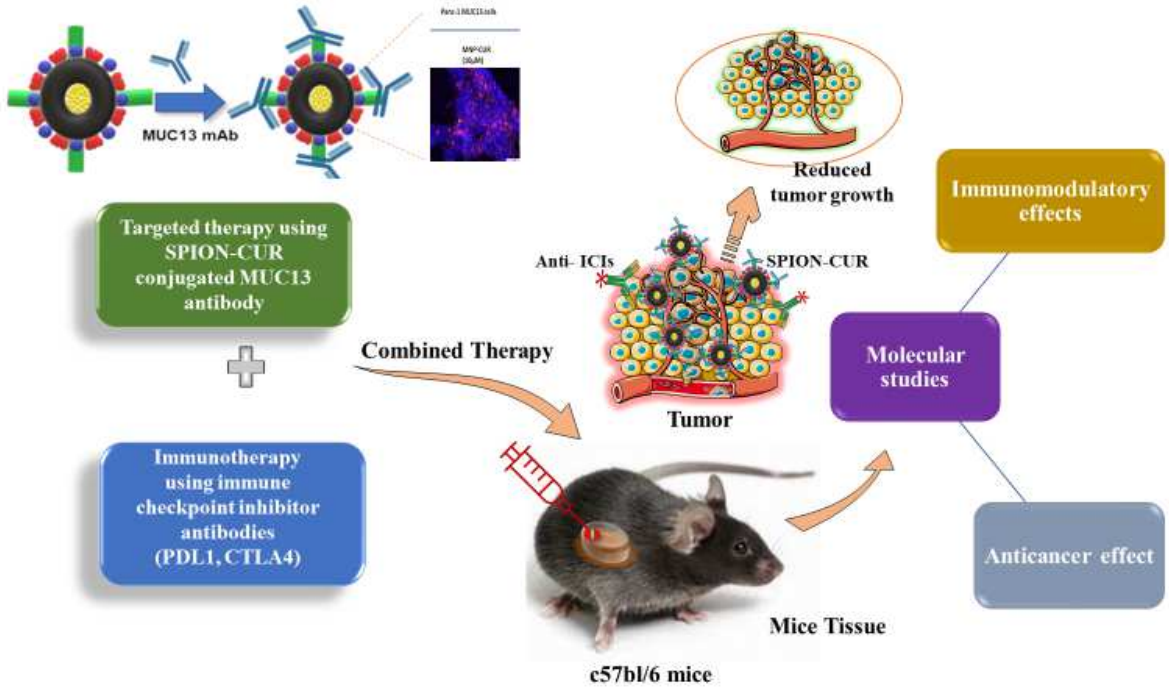

Fig. 18. Schematic representation of the proposed study. The SPION-CUR conjugated MUC13mAb in combination with immune checkpoint inhibitors, PDL-1 and CTLA4 will be administrate in female c57bl/6 mice model with KPC primary tumor. Tissues and organs from the mice will be collected for further analysis.

2. MATERIALS AND METHODS

2.1 Chemicals, reagents, and antibodies:

All chemicals and reagents were purchased from Sigma Aldrich Corporation (St.Louis, MO, USA) and cell culture wares were purchased from Corning life sciences (Tewksbury MA, USA). The antibodies Ly-6CmAb (# 47-5932-82), CD8amAb (# 15-0081-82), Ly-6GmAb (# 61-9668-82), CD27mAb (# 11-0271-82), CD45mAb (# 67-0451-82), CD4mAb (# 61-0042-82), CD25mAb (# 35-0251-82), F4/80mAb (# 62-4801-82). Immune checkpoint antibodies, anti-mouse PDL-1 (B7H1) (#BE0101), anti-mouse CTLA-4 (CD152) (#BE0131) and polyclonal human IgG (#BE0092) from BIO-X-cell. Tissue storage solution (MACs media, lot no# 130-100-008).

2.2 Stable transduction of luciferase gene in KPC Cells for bioluminescence

Cells were maintained at 37°C and 5% CO2 incubator with 95% air atmosphere and cultured in DMEM/F12 (Gibco.) medium, supplemented with 10% fetal bovine serum (Gibco.), 1% antibiotic and antimycotic solution. Stably expressing lentiviral luciferase cells, HPAF-II and KPC were generated in the lab. Briefly, the cells were treated with a range of doses of antibiotic to determine the lowest dose that kills all of the cells. Lentiviral transduction was performed using pre-packaged virus. Luciferase activity was checked every 2 weeks using XenoLight (PerkinElmer #122799).

2.3 Animal handling and Survival surgery in C57BL/6J mice

8 weeks old female C57BL/6J mice form Jackson Laboratories used for animal experimentation. All the protocols were approved and reviewed by University of Texas Rio

Grande Valley Institutional Animal Care and Use Committee (UTRGV-IACUC: AUP-20-15).

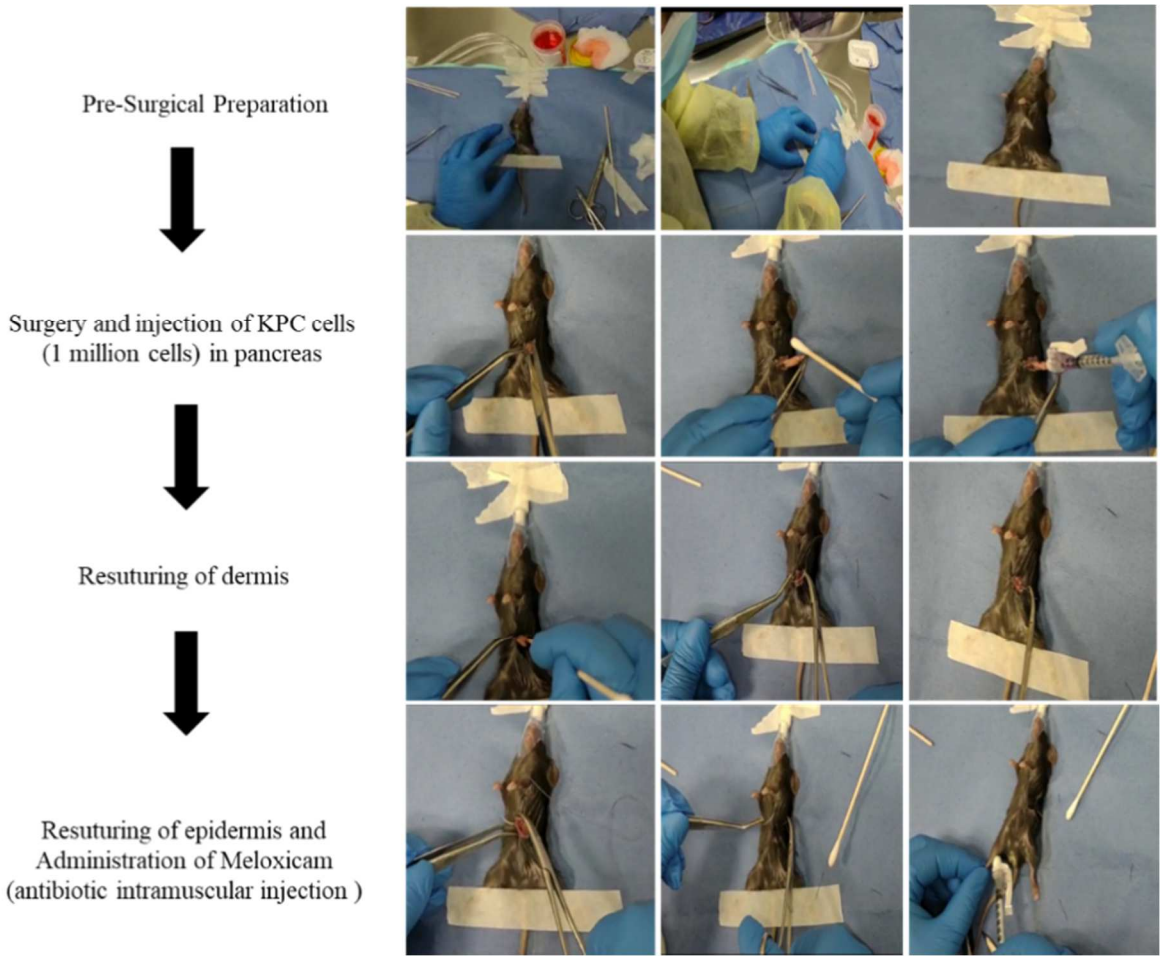

Fig. 19. Survival surgery was performed 8-week-old female C57BL/6J black mice.

Mouse pancreatic cancer cell line, KPC luciferase [1 x 106 cells/ml in a 1:1 mixture of chilled Matrigel:Phosphate buffered saline (1X PBS)] was used in this study. Luciferin will be transfected into these cells for the purpose of bioluminescence animal imaging. C57BL/6J mice (6–8-week-old) will be placed into the following groups and injected with mouse pancreatic cancer cells (suspended in 50ul PBS) orthotopically in mice using following procedures followed by drug treatments through intravenous route. ***Preparation of pancreatic Cancer Cell Lines for***

implantation: Stably expressing lentiviral luciferase cells, KPC was used. These transduced pancreatic cancer cells were cultured until 70% confluent and was lifted with viability greater than 90%. Cells were resuspend at 1 x 10^6 cells/ml in a 1:1 mixture of chilled Matrigel:Phosphate buffered saline (PBS). The KPC cell line is known to grow rapidly, and this cell number is a guide and may change for each cell line.

Preparation of mouse: Mouse was anesthetized using inhalation of 2-3% isoflurane. The depth of anesthesia was determined by lack of pedal reflex to a gentle toe pinch. Lubricant was applied to the eyes to prevent desiccation. Mouse was positioned on its back on a 37 °C heating pad and gently turned the mouse to raise the left side of the abdomen. Abdomen was swiped with a 10% povidone iodine solution. ***Laparotomy:*** Using a sterile surgical instrument, a 1.5 cm incision was made in the skin approximately 1 cm left lateral from the midline. Followed by a 1.5 cm incision in the underlying abdominal muscle. The spleen was located using the forceps and gently removed from the abdominal cavity. The spleen was secured along a sterile cotton bud to expose the underlying pancreas. Pancreas tail was located adjacent to spleen using the forceps and gently took out the underlying pancreas. Using a 29 G 0.3 ml insulin syringe, we have injected 20µl of the Matrigel-cell suspension into the pancreas. Following injection, we hold the syringe in the pancreas for 30-60 sec until the Matrigel has solidified. This important step which can minimize cell leakage. Site of injection was inspected to ensure no leakage occurred. The spleen and pancreas were placed into the abdominal cavity. ***Abdominal Wall Closure:*** Abdominal musculature of the mouse was closed with an absorbable braided 4-0 suture with a round needle using a continuous stitch. Followed by the closure of the external skin with a non-absorbable monofilament 6-0 suture with a cutting needle using a continuous stitch. Mouse was removed from the inhaled anesthetic and injected 0.05-0.1 mg/kg meloxicam

subcutaneously (30 µl). Mouse was placed on a 37 °C heating pad with free access to food and water for recovery. If mice demonstrated signs of pain such as hunching or reduced mobility, meloxicam was given every 12hrs over a 36hrs period. Mice were monitored for regular breathing and the ability to respond to touch. Mice was rotated from side to side every 15 minutes until they were able to maintain sternal recumbency. Mice was monitored daily during the health checks for any changes in behavior, such as anorexia, reluctance to move, etc. Analgesics recommended dose was given as needed. Any animal experiencing an adverse reaction or improper injection was removed from study and euthanized. After tumor implantation, all mice were monitored for the tumor growth and general signs of morbidity such as ruffled fur, hunched posture, and immobility.

2.4 Preparation of formulation and Treatment Strategy

Preparation of formulation: 10 mg/ml of SPION stock was first prepared (Khan et al., 2019). Curcumin (2 mg) was loaded to 20 mg/2 ml of SPIONs to form 2 mM SP-CUR (10:1) formulations. Reaction parameters for loading curcumin into SPIONs include overnight incubation at 4 °C temperature under stirring conditions on a magnetic stir plate (500 rpm). Next day SPION-CUR was washed 3 times using distilled water by magnetic pull method to remove any unbound SPION-CUR. 1mg of SPION-CUR was pulled using magnet and added with 800µl of 10mM sodium bicarbonate under stirring at 500rpm. Meanwhile 1 mg of PEG succinimidyl ester linker, MW 5000 (NANOCS, NHS-PEG-NHS) was dissolved in 200 µl 10 mM sodium bicarbonate. 1mg of NANOCS, NHS-PEG-NHS was added dropwise under stirring condition to 1mg of SPION-CUR formulation for an hour. The unreacted linker was removed by washing using magnet and activated NHS linked SPIONs were again suspended in PBS. In second step,

100 µg of MUC13mAb was slowly added at 4□ for 18hrs to generate MUC13 targeted SPIONs. The unconjugated MUC13mAb was removed by washing using magnet at room temperature for 1hr. For SP-CUR IgG, in the second step 100 µg of IgG mAb was slowly added with same condition. ***Treatment Strategy:*** The model developed tumor within a week and sorted randomly for 7 treatment groups (N= 5), which include, Group 1: SPION (control), Group 2: SPION-CUR-IgG, Group 3: SPION-CUR-MUC13, Group 4: PDL-1, Group 5: CTLA-4, Group 6: SPION-CUR-MUC13+PDL-1, and Group 7: SPION-CUR-MUC13+CTLA-4. Treatments started at day 7 after surgery (n=5 mice per group). Drug treatments was done through intraperitoneal route; Control group (SPION and isotype IgG control, one time a week, i.p.), SPION-CUR-MUC13 group (100µg SP-CUR-M13, one time a week, i.p.), anti-PD-L1 group (100 µg anti-PD-L1/mouse, once a week, i.p.), anti-CTLA-4 group (100µg anti-CTLA-4/mouse, once a week, i.p.) and combination treatment groups (concurrent treatment of SPION-CUR-MUC13 with anti-PD-L1and anti-CTLA-4 respectively). 100 µg/mice of SPION formulations were injected to each mouse groups intraperitonially once a week for 4 weeks except second week when the treatment was given twice a week. Imaging was done every week and mice were monitored for death. The tumor and organs were collected for further molecular studies.

2.5 Bioluminescent Tracking of Pancreatic Cancer Progression and mice sacrifice

Mouse was anesthetized using inhaled isoflurane. For tracking the KPC luciferase cancer progression 150 mg/kg D-luciferin was injected via tail vein. Bioluminescence image was captured using bioluminescent imaging system by placing the mouse inside the case with sufficient oxygen supply. Mouse was removed after capturing the image and allowed to recover in its home cage. (Note: Bioluminescent imaging is non-invasive and can be conducted

periodically to investigate tumor growth kinetics. To image tumor in the pancreatic tail, it is important to put the mouse on its left side, so the tumor points towards the camera). We imaged the mice using IVIS Spectrum scanner (PerkinElmer, Waltham, MA) at the UTRGV, Biomedical research core facility, running Living Imaging 4.3.1 software with binning 4, FOV 12.5, F-stop 1, exposure 1 - 60 sec (determined by the highest exposure without pixel saturation). Mice was be sacrificed at 5th week and the presence of fluorescence in tumors, and organs was determined using the Animal Imager. Increased tumor size and metastases (and/or increased fluorescence) in certain group(s) compared to others was determine the effectiveness of drugs in inhibiting tumorigenesis.

2.6 Flow Cytometry

Tissue Dissociation and Preparation of Single Cell Suspension: Single cell suspension was prepared from tumor tissue stored in MACs tissue storage solution. Tumor tissue with a size of 2- 4mm was cut into small pieces and transferred to gentle MACs C tube containing enzyme mix (Tumor dissociation kit protocol #). Tumor was dissociated using Gentle MACs^{TM} octo dissociator with heater and enzymatic treatment to produce single-cell suspensions with high viability and a high degree of standardization for reproducible results. MACS® Tissue Dissociation Kits are designed to extract high yields of viable single cells with intact epitopes from almost any type of solid tissue. Red blood cell lysis solution was used to ensure minimal effect on all cell types obtained from tissue sample. One volume of cell suspension was diluted with ten volumes of 1X RBC lysis solution. (Example: 1ml cell suspension with 10 ml of 1XRBC cell lysis solution). Cells were vortexed for 5seconds and incubated at room temperature

for 2-3minutes, preferably 5minutes. After the incubation cells were centrifuged at 300 X g for 10minutes at room temperature and discarded the supernatant. ***Staining of Cell Suspension:***

Cell pellet was washed with 1ml of 1X PBS by centrifugation at 350 Xg for 7minutes at 4□. After washing cells were resuspended in 1ml of 1XPBS and cells were counted. The density of cells was adjusted to 1 x 10^6 cells in 1 ml volume. To this 1 µl of reconstituted fluorescent reactive dye was added and mixed well. Fluorescent reactive dye was prepared by mixing component A (fluorescent reactive dye) with component B (anhydrous DMSO). Cells were incubated at room temperature for 30minutes. (Note: light sensitive). After incubation, wash the cells with 1X PBS by centrifugation at 350 Xg for 7minutes at 4□ and discard the supernatant. 100 µl volume of supernatant residue was kept back.

Fixation and Permeabilization of Cell Suspension: Cells were fixed by adding 100 µl of IC fixation buffer and pulsed vortexed the mixture. Fixed cells were incubated for 35minutes at room temperature (Note: Light sensitive). After the incubation period cell suspension was washed twice with 1ml of 1X PBS at 450 Xg for 5minutes at room temperature. The supernatant was discarded and at this stage the cell pellet could be stored in 5% FBS and 95% 1X PBS, at 4□ for 2-3 days. The fixed cells then stained with cell surface markers and permeabilized with 1X permeabilization buffer. The cell- antigen was resuspended in flowcytometry staining buffer for flow analysis (~1 million cells/flow). Immuno-profiling was performed for all 7 treatment groups for two antibody panels. Panel contains 11 antibodies: F4/80, CD11b, CD45, CD27, CD44, Ly6G, CD8, CD45RB, CD3, Ly-6C, and CD25, FOXP3, CD4, CD25, and CD3. Flowcytometry was performed using Attune flow cytometer.

2.7 Immunohistochemistry

MACH 4 Universal HRP Polymer detection kit was used to perform immunohistochemical analysis for immune checkpoint inhibitor proteins (anti-PDL-1, anti-CTLA-4) and tumor stromal protein (α-SMA). Immunohistochemistry was performed on formilin fixed, paraffin embedded orthotopic mouse tumors (5 m slices) (Biocare Medical; Concord, CA). The tumor tissues were deparaffinized, rehydrated, treated with 0.3 percent hydrogen peroxide, and processed for antigen retrieval. The samples were processed for staining to analyze the expression of designated proteins in the tissues after blocking with background sniper. Then the slides were counterstained for hematoxylin, dehydrated, and mounted with VectaMount (Vector Laboratories). The mounted slide was scanned under ScanScope® XT/XT2 system (Aperio, Vista, CA).

2.8 Prussian blue staining for SPION detection in extracted mice tissues

Formalin-fixed paraffin-embedded (FFPE) tissue slides from orthotopic mice were deparaffinized, rehydrated and proceeded for Prussian blue staining. Tumor tissues from SPION containing groups (n=2) were stained and incubated with a mixture of 2%potassium ferrocyanide, 2% hydrochloric acid (30 min). After 30 min the tissue slides were washed 3 times with PBST and mounted. The images were captured using slide scanner to determine the uptake of iron particle inside the Tissue.

2.9 Immunoblotting assay

To make the protein lysates from tumor tissues, 25 mg tissue was homogenized in RIPA lysis buffer using a tissue homogenizer, then centrifuged at 12,000 rpm for 10 minutes. The protein concentration in the supernatant was measured using the Bradford test, then resolved on

SDS-PAGE and immunoblotted. Anti-PDL-1, anti-MUC13CTLA-4, and anti-–actin antibodies were used to evaluate protein expression by immunoblotting.

3. RESULTS

3.1 Successful stable transduction of KPC lentiviral cells show bioluminescence

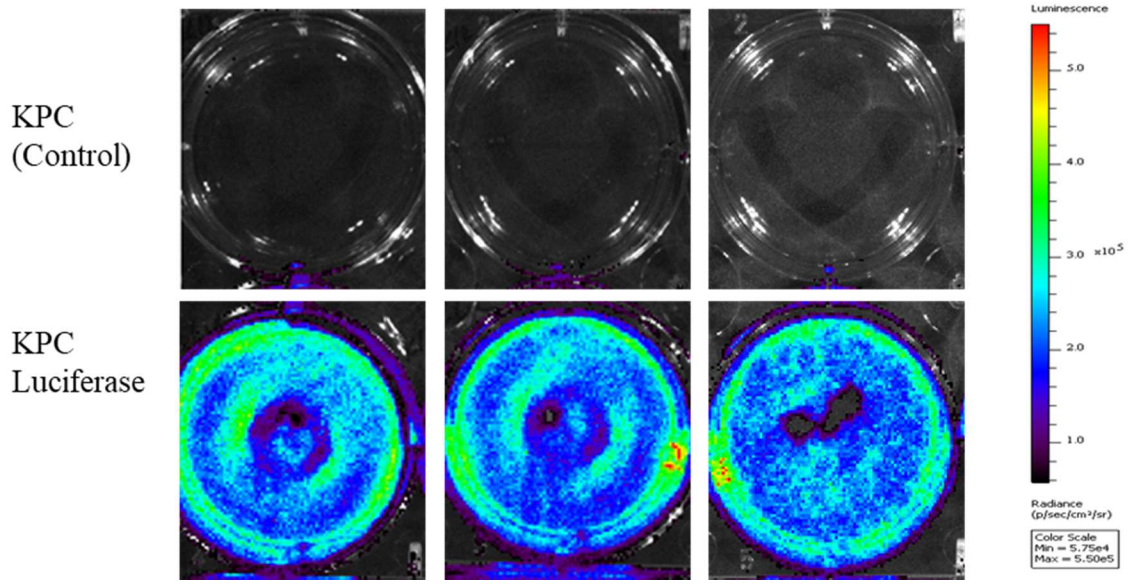

Fig. 20. Bioluminescence imaging in KPC Luciferase cell line. Luciferase activity of KPC luciferase cell was tested using XenoLight Bioluminescent/Chemiluminescent Substrates PerkinElmer. Normal KPC mouse pancreatic cell was used a control.

KPC cell line is an established and significant model for studying pancreatic ductal

We have used KPC mouse generated cell line (*LSL-Kras*^{G12D}*; LSL-Trp53*^{R172H}*; Pdx1cre*) for developing syngeneic orthotopic xenograft mouse model of PDAC using C57 black mice. KPC mouse model recapitulates the disease progression seen in humans, such as initiation of PanCa

with mPanINs, followed by progression to invasive adenocarcinoma, and subsequent metastasis into distant organs. It has a point mutation in transformation related protein 53 gene (TP53R172H), and in the KRAS gene (KRASG12D) that generate non-functional proteins. Metastases is seen in 80% of KPC mice model located primarily in lung and liver. Thus, orthotopic mice model with KPC tumor will be a good study model to study both localized and metastases tumors. The cells demonstrated excellent bioluminescence as seen using plate reader (Fig. 20.). This KPC luciferase cells when injected in pancreas can track the tumor growth and metastasis that will help us to determine the effect of the treatment. KPC luciferase were cultured in large scale and checked for its luciferase activity using PerkinElmer's XenoLight substrate.

3.2 MUC13 conjugated SP-CUR combination treatment improved CTLA-4 and PDL-1 checkpoint therapy in -*Kras*^{G12D}; *LSL-Trp53*^{R172H} syngeneic mouse model of PDAC

Previous reports on the SPION-CUR used in our study have demonstrated its efficacy in inhibiting the tumor stroma and desmoplasia, which makes the tumors soft to overcome barriers associated with drug delivery (Khan et al., 2019). This is a very common especially in advance pancreatic tumors, which makes the tumors highly resistant to therapies. Therefore, we evaluated the efficacy of MUC13 conjugated SP-CUR on the PDL-1 and CTLA4 checkpoint immune therapies. We observed that the mice treated with SP-CUR died earlier than the mice treated with MUC13 conjugated SP-CUR. This signifies that MUC13 conjugation improved the efficacy of SP-CUR. Mice treated with SP-CUR-M13+CTLA-4 had longer survival in comparison with CTLA-4 alone and vehicle-treated mice (Fig. 21 and Fig. 22. A). Most importantly, out of 5 mice, 2 mice survived until the end of the study and had no tumor. These mice had significant hair loss and thickening of blood, which was observed at the time of blood collection. These two

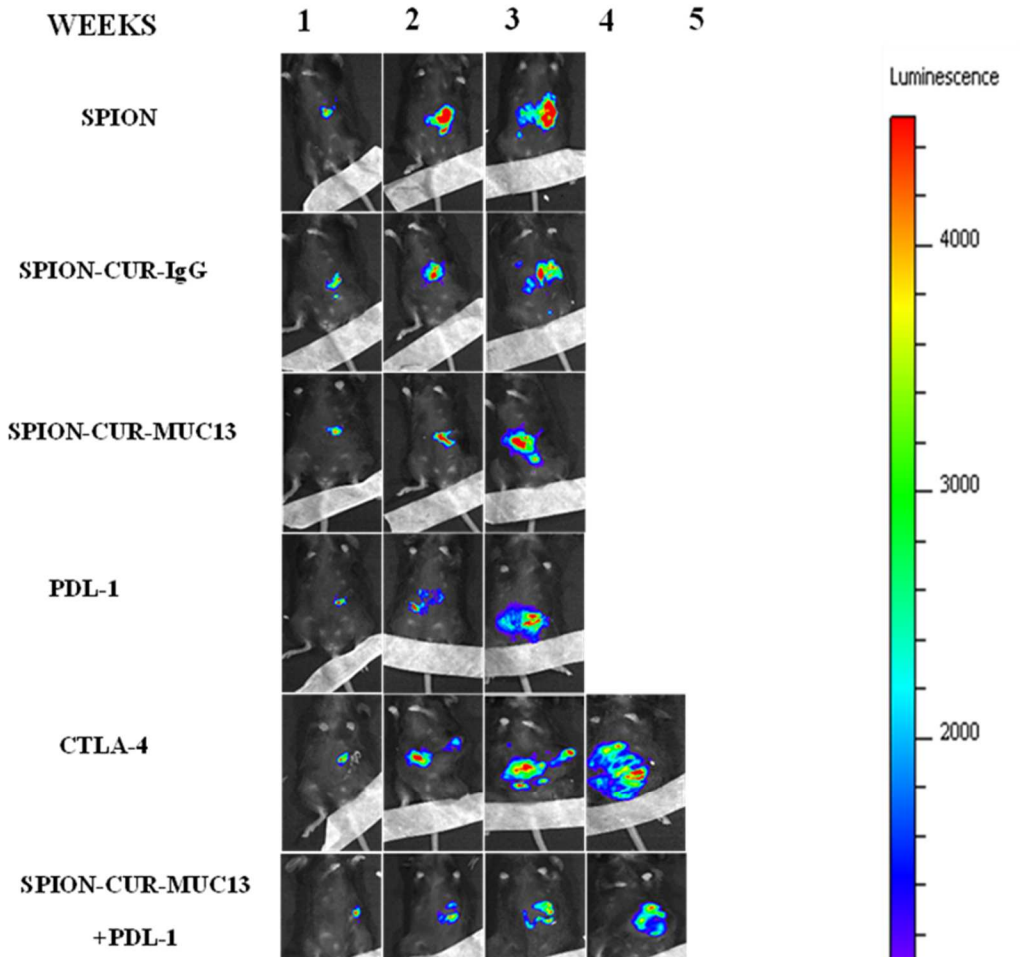

Fig. 21. Luciferase labelled KPC cells (1×10^6) were orthotopically implanted in C5BL6 mice. Treatment started 7 days post□implantation with five mice per group. Bioluminescence imaging of live mice was performed at the indicated weeks as described in the Methods section. All images were displayed at the same scale.

survived mice from SP-CUR-M13 +CTLA-4 group were sacrificed when all mice from rest of the groups reached endpoint (abdominal diameter of ≥35 mm) or died. Mice treated with SP-CUR-M13 in combination with CTLA-4 had significantly lower tumor burden (70%) in

comparison with CTLA-4 alone (<0.05) and vehicle-treated mice ($p<0.0005$) at death. Almost 70% mice treated with CTLA-4 and PDL-1 alone had formation of ascites, which was less when combined with SPION-CUR-MUC13. But this could be probable reason of death in some mice from SPION-CUR-MUC13 +CTLA-4 group and SPION-CUR-MUC13 +PDL-1 group. Similar results were observed with SPION-CUR-MUC13+PDL-1 combination therapy, although the reduction in tumor burden was approximately 60% in comparison with PDL-1 alone (<0.05) and vehicle-treated mice ($p<0.0005$) (Fig. 22. B).

SPION-CUR and SPION-CUR-MUC13 had no significant effect on improved survival. Additionally, our results clearly signify that combination treatment of checkpoint therapies improved survival, reduced ascites formation and tumor burden in the KRAS Trp53−/− mouse model. These results suggest the potential therapeutic benefit of the addition of SPION-CUR-MUC13 in immune checkpoint treatment of PDAC.

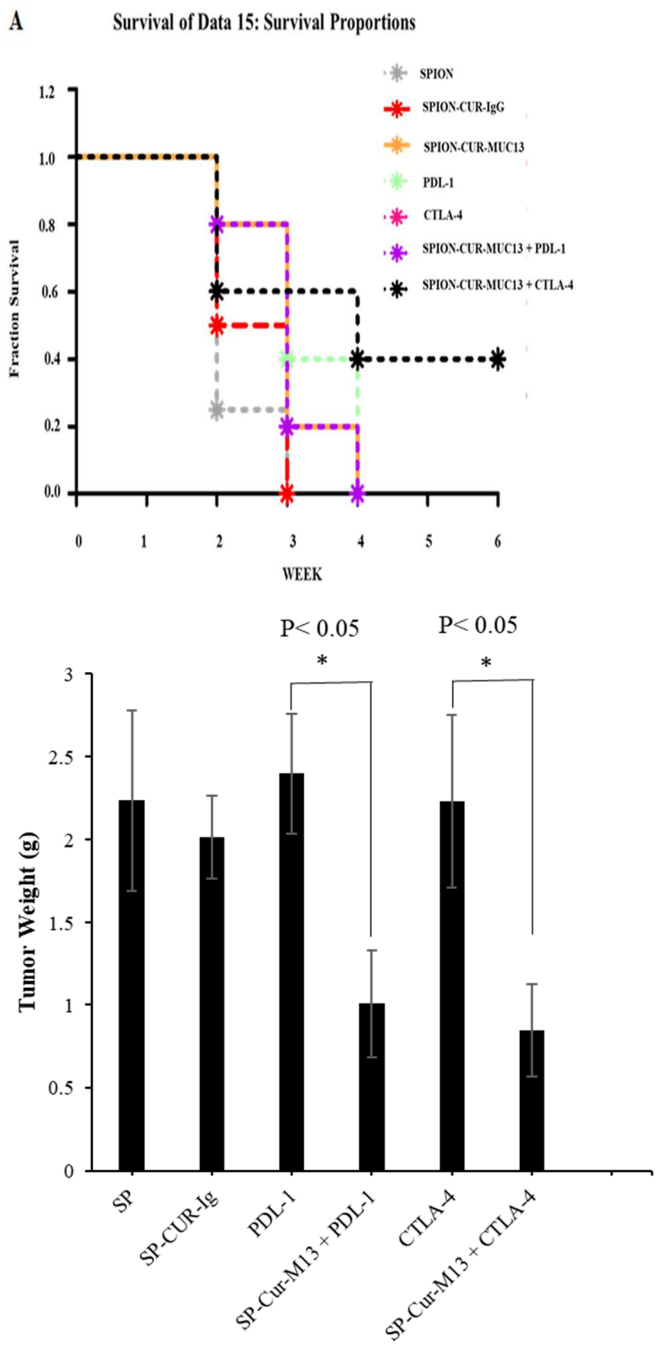

Fig. 22. Tumor Survival Curve and Tumor Weight (A) Survival curve represent the effect of combined therapy of SPION-CUR in combination with CTLA-4 and PDL-1 checkpoint therapy (B) Treatments showed significant reduction in tumor growth in combinations. P<0.05, this difference is considered to be statistically significant.

3.3 SP-CUR reprogrammed myeloid cells, regulatory T cells (Tregs) to overcome TME-instigated resistance mechanisms to checkpoint immunotherapy

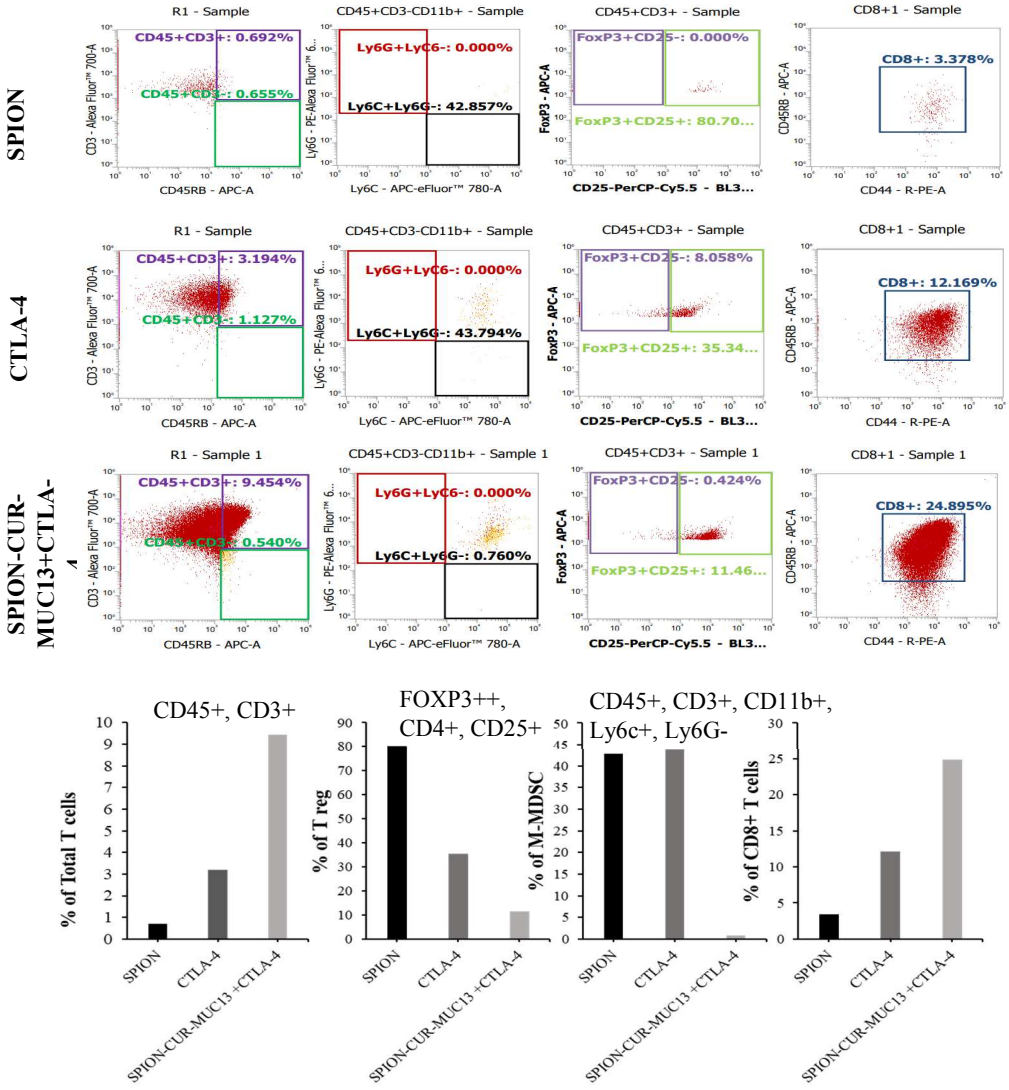

Fig. 23. Flow analysis for investigating the immunostimulatory effect of SP-CUR-M13 in combination with CTLA-4. The SPION-CUR in combination with CTLA-4 showed increased T-cell infiltration and decreased immunosuppressive cells; Treg and M-MDSC.

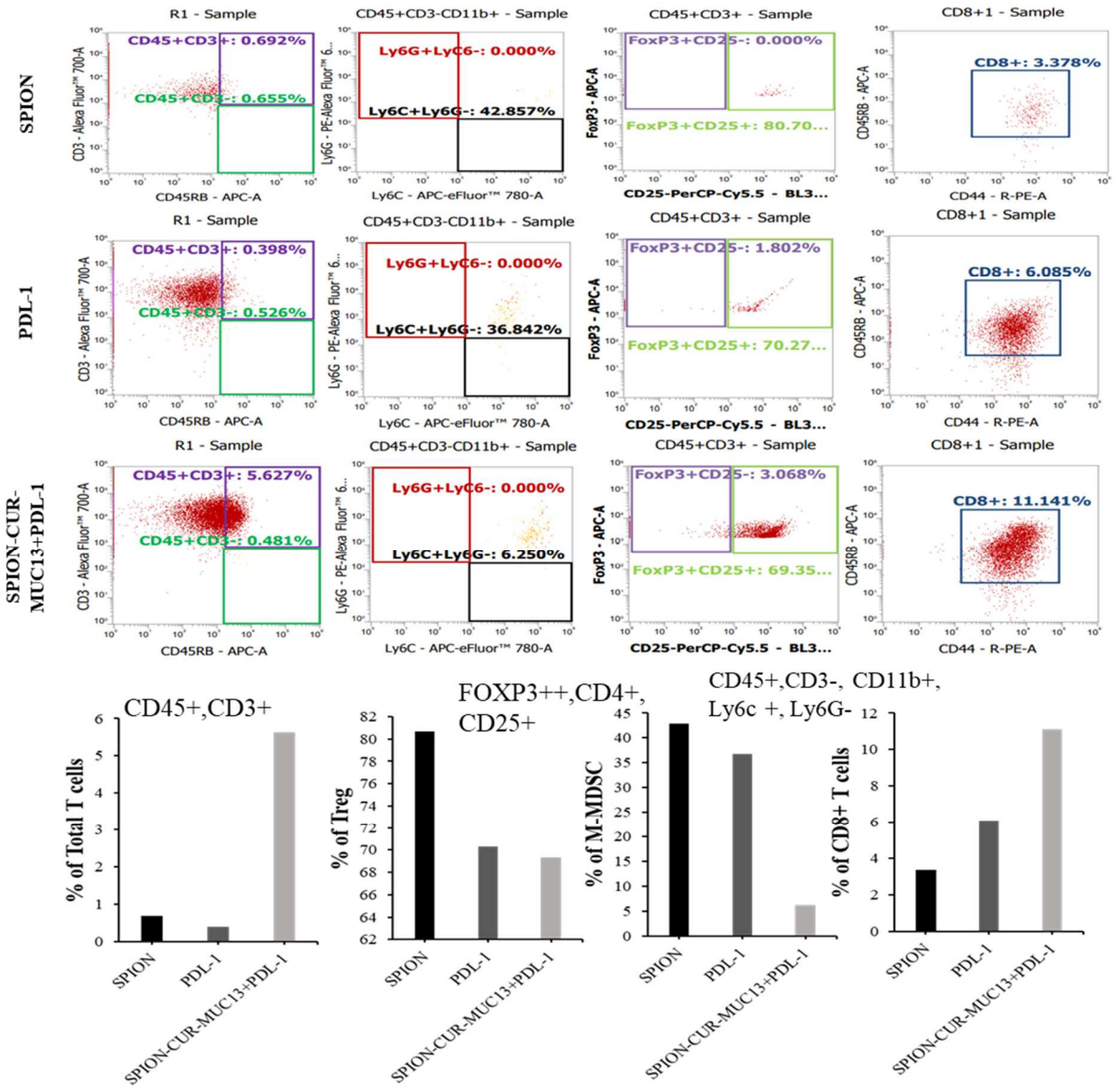

Fig. 24. Flow analysis for investigating the immunostimulatory effect of SP-CUR-M13 in combination with PDL-1. The SPION-CUR in combination with PDL-1 showed increased T-cell infiltration and decreased immunosuppressive cells; Treg and M-MDSC.

Chemotherapeutic drugs exert immunostimulatory effects, either by inhibiting immunosuppressive cells and/or activating effector cells, or by increasing immunogenicity and

increasing T-cell infiltration. Vehicle-treated group, PDL-1 and CTLA-4 alone showed significantly increased levels of myeloid-derived suppressor cells (mMDSCs) i. e $CD45^+$, $CD3^-$, $CD11b^+$, Ly6C high, $Ly6G^-$ and T-Regulatory cells (Treg) ie. $FoxP3^+CD25^+CD45^+CD3^+$ cells in $Kras^{G12D}$; $LSL\text{-}Trp53^{R172H}$ syngeneic mouse model of PDAC (Fig. 23. & 24.). Interestingly, the combined treatment of SP-CUR-M13 with CTLA-4 reduced the population by 43% and 23.8%, respectively (Fig. 23.). Similar results were observed in SP-CUR-M13+PDL-1 group, which showed reduction in MDSCs (by 26.6%) and Tregs (by 0.1%) as compared with PDL-1 alone (Fig. 24.). These data confirm that effects of SP-CUR-M13 on immune checkpoint expression on myeloid cells and thus provide the rationale for combination treatment with PD-L1/CTLA4 immune checkpoint blockade. Additionally, reduced immune tolerance, increased infiltration of total T cell population and CD8+T cells are observed in mice treated with combination checkpoint regimen.

3.4 SP-CUR-M13 specifically targets pancreatic tumor in $Kras^{G12D}$; $LSL\text{-}Trp53^{R172H}$ syngeneic mouse model of PDAC

MUC13 conjugated SP-CUR was investigated for tumor specific delivery in syngeneic mouse model of PDAC. For this study, we selected orthotopic ***$Kras^{G12D}$; $LSL\text{-}Trp53^{R172H}$*** **syngeneic mouse model of PDAC and a no tumor control mice.** Indocyanine Green (ICG) labeled anti-MUC13 MAb was injected intraperitoneally in tumor bearing and a no-tumor bearing C57 Black mice for 3hrs. The (ICG) labeled anti-MUC13 MAb was able to specifically target the mice bearing KPC tumors as depicted by green ICG fluorescence, while a no-tumor

bearing mice did not show any fluorescence. These results depict that MUC13 is able to target the ***Kras^{G12D}; LSL-Trp53^{R172H}*** **syngeneic mouse model of PDAC (Fig. 25.).**

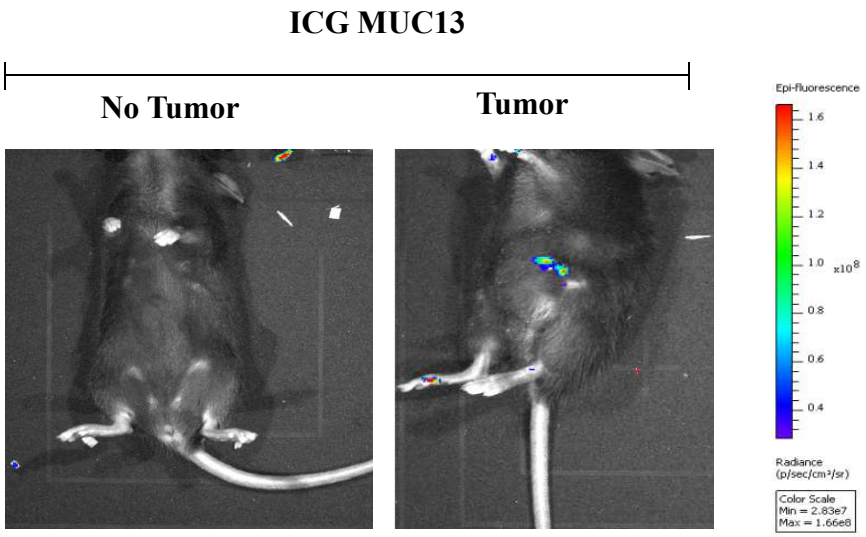

Fig. 25. Targeting efficacy of SP-CUR-M13. Pancreatic tumor specific targeted delivery of Indocyanine green (ICG) labelled SP particles with MUC13 (Targeted SP-ICG-MUC13) in *Kras^{G12D}; LSL-Trp53^{R172H}* syngeneic mouse model of PDAC.

3.3 SP-CUR-M13 internalizes pancreatic tumors of *Kras^{G12D}; LSL-Trp53^{R172H}* syngeneic mouse model of PDAC and inhibits tumor stroma

The excised organs, including pancreas tumor of mice was subjected to Prussian staining to investigate the internalization of SP-CUR-M13. SPION intake was seen in the treatment groups; control group (SPION and SPION-isotype IgG control), SPION-CUR-MUC13 group, and combination treatment groups (SPION-CUR-MUC13 with anti-PD-L1and anti-CTLA-4 respectively). The staining for Prussian blue illustrates the cell uptake of SPION formulation in the mice model (Fig. 26.).

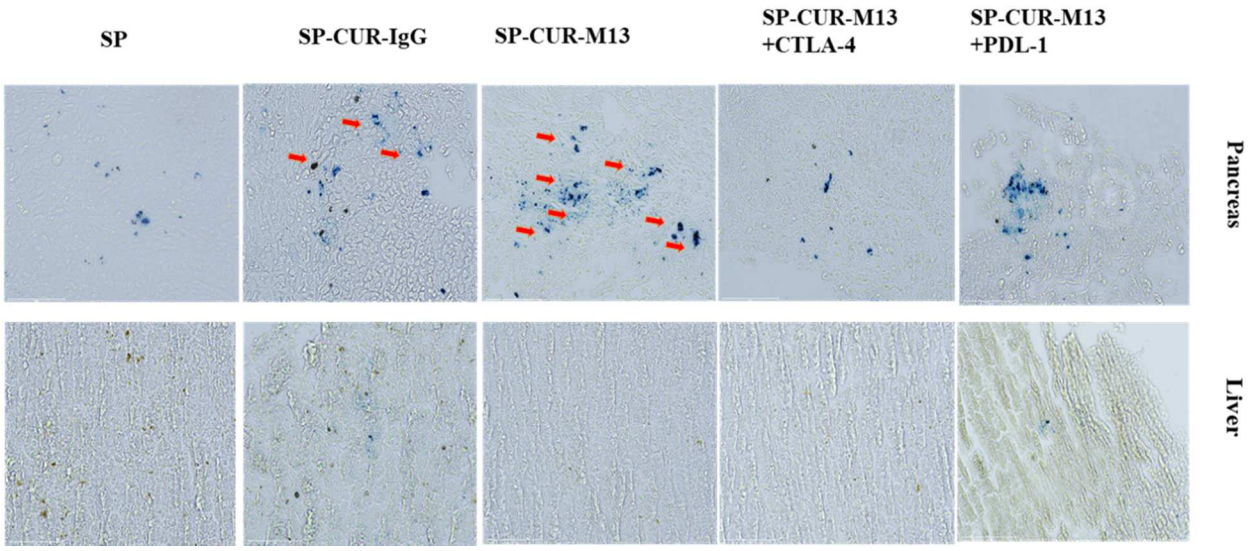

Fig. 26. Prussian blue staining depicting the uptake of SPION nanoparticle in the excised body organs from *Kras*^{G12D}*; LSL-Trp53*^{R172H} syngeneic mouse model of PDAC.

We also sought to investigate the effect of treatment on PDL-1 and CTLA-4 expression. Changes in the expression of CTLA-4 and PDL-1 were analyzed using Immunohistochemistry (brown). Both the expression of PDL-1 and CTLA4 was inhibited in presence of combination treatment with SP-CUR-M13 (Fig. 27.). These results further confirm the inhibition of PDL-1 and CTLA-4 checkpoints and explains the improved therapy in our experiment.

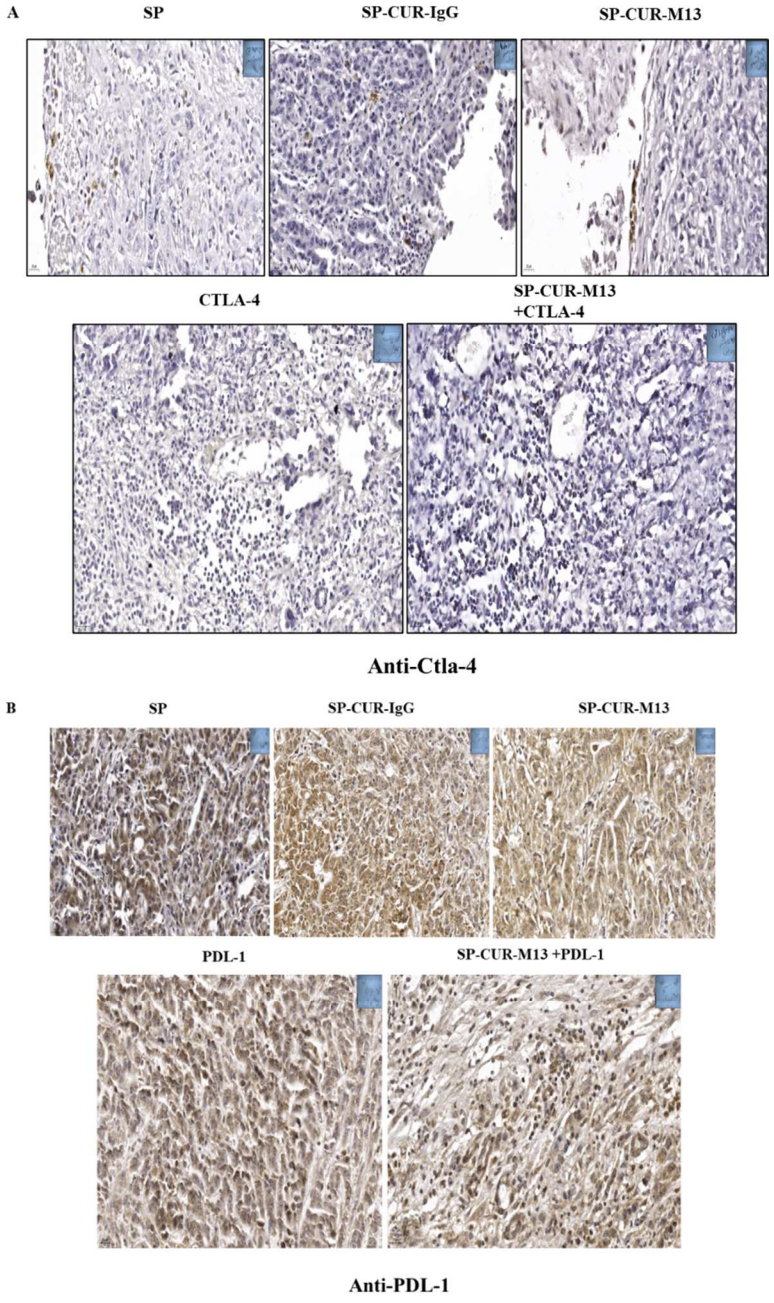

Fig. 27. Immunohistochemical staining showing the inhibited expression of (A) CTLA-4, (B) PDL-1 in tumor mice tissue. Expression of SP-CUR-M13 in combinations was analyzed using Immunohistochemistry (brown).

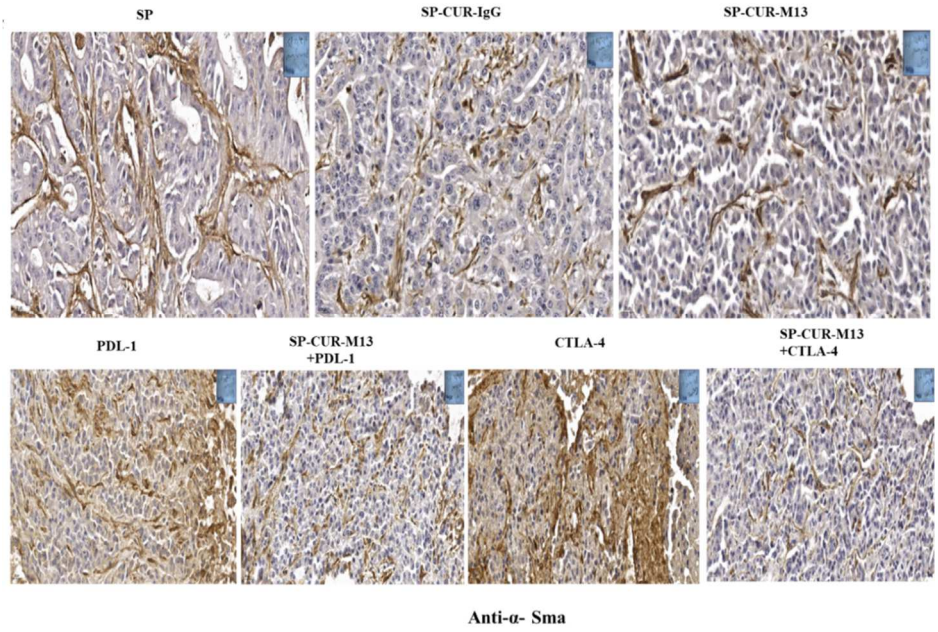

Fig. 28. Formalin-fixed paraffin-embedded (FFPE) tissue slides from treated orthotopic mice were deparaffinized, rehydrated and proceeded for immunohistochemistry. Changes in the expression of α-sma was analyzed using Immunohistochemistry (brown)

These changes are the consequence of stroma targeting ability of SP-CUR-M13 as confirmed by the inhibition of an important protein of tumor stroma, α-SMA that was observed in the tumor tissues of mice that was treated with combination regimen (Fig. 28). The stroma targeting ability of SP-CUR has been already proven and demonstrated in the publications from mentor's lab (Khan et al., 2019).

3.8 Combination Therapy with SP-CUR Inhibited CTLA-4 and PDL-1 in pancreatic tumors of *Kras^{G12D}; LSL-Trp53^{R172H}* syngeneic mouse model of PDAC

Whole lysate was prepared from all the seven treatment groups SPION, SPION- isotype IgG control, SPION-CUR-MUC13, anti-PD-L1, anti-CTLA-4 group and combination treatment groups (SPION-CUR-MUC13 with anti-PD-L1and anti-CTLA-4 respectively). Further, immunoblotting was performed for the antibodies (A) PDL-1 (Immune checkpoint protein) (B) CTLA-4 (Immune checkpoint protein) and β-actin as loading control (Fig. 29 A & B).

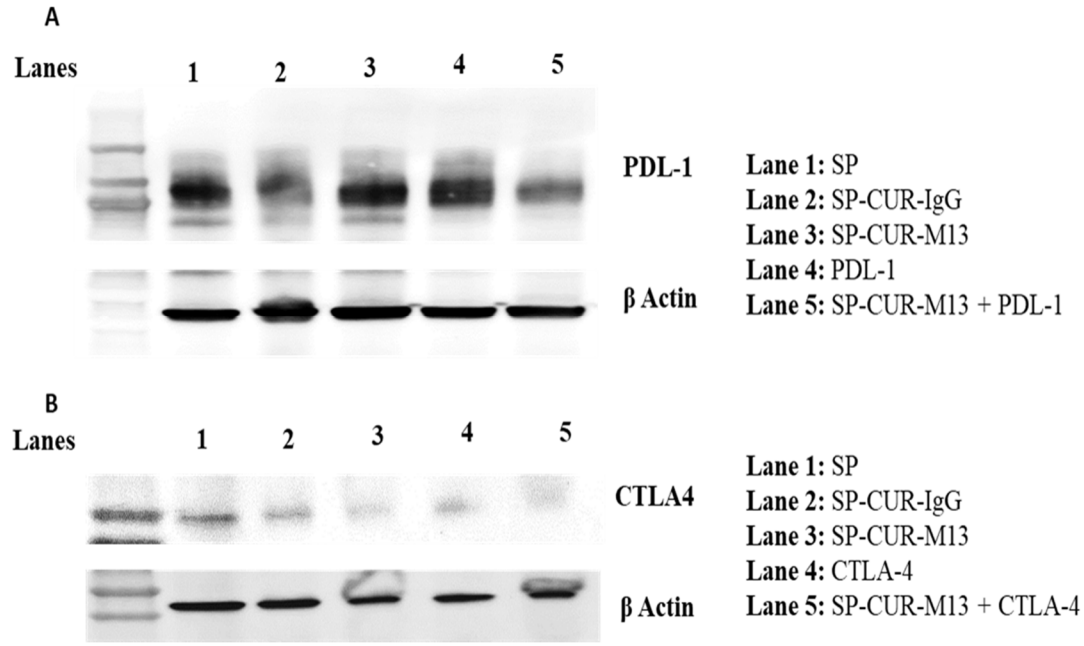

Fig. 29. Western blotting analysis indicating the effect of combination therapy with SP-CUR in(A) PDL-1 and (B) CTLA-4; beta-actin (control) of excised tumor lysates (pulled) from all seven groups.

Immunoblotting analysis data suggested that SPION-CUR in combination with CTLA-4 inhibitor clearly downregulated the expression of CTLA-4. This data supports the longer survival rate of mice given with combination of SPION-CUR and anti-CTLA-4 when compared to single therapy of anti-CTLA-4 or anti-PDL-1.

4. DISCUSSION

Pancreatic cancer remains to be 3rd deadliest disease with aggressive malignancy, poor therapeutic response and chemoresistance. The 5 years survival is only 6-10% and 10-15%patient considered for surgery, due to lack of early diagnosis. MUC13, which is a recently identified mucin glycoprotein, is aberrantly expressed in pancreatic tumors has a tremendous tumor targeting ability and may serve as an excellent target for Pancreatic cancer treatment. ABRAXANE in combination with gemcitabine is the current first line treatment for PDAC and are limited to patients with advanced and metastatic adenocarcinomas of pancreas. Immunotherapy has shown promising results in other cancers but limited response in pancreatic cancer due to desmoplasia and fibrotic tumor microenvironment. Combinatorial targeted therapy along with immunotherapy could be an effective therapeutic modality. At the same time, successful translation to the clinic by efficient delivery of therapeutic molecules to the target pancreatic tumor stroma is a major challenge. Therefore, this study describes a novel engineered super paramagnetic iron oxide nanoparticle (SPION) formulation to deliver Curcumin (principal curcuminoid of turmeric, *Curcuma longa*) to overcome the desmoplasia and deplete tumor stromal resistance.

Our first goal was to generate and characterization of the formulation (SPION-CUR-MUC13). Size of the final formulation is 115.9 nm and zeta potential -21.39 mV, which suggest an ideal delivery vehicle for cancer therapy. In our previous research article, we have used this SPION formulation to deliver curcumin to PanCa cells, this unique did not show any toxicity to normal cells, cancer cells, RBCs, and they exhibited hemocompatibility(Khan et al., 2019). Anti-PD1 (pembrolizumab and nivolumab) immunotherapy for solid cancer with MSI-h or mismatch repair deficiency are in use (Boyiadzis et al., 2018; Yoon et al., 2021a) while other

immune checkpoint inhibitors are in clinical trials. Pancreatic tumor microenvironment is being the hot spot for fibrotic stroma is the main reason for the poor success rate of immunotherapy. The tumor microenvironment variety of cells (stellate cells, pan-endothelial cells, and infiltrating immune cells such as MDSC, Treg cells, and tumor-associated macrophages) and extracellular matrix (ECM) components with blood vessels and nerves. To overcome this physical barrier will be the greatest challenges. Therefore, development of newer strategies to enhance immunotherapy is required, Wherein, tumor stroma can be depleted using combined drugs for improved tumor response to immunotherapies. Here we are combining our MUC13mAb conjugated SPION-CUR with immune checkpoint inhibitors (anti-PDL-1 and anti-CTLA-4) that can deplete the stroma and soften up tumors for improved immune response. This combination treatment was performed using orthotopic mice model by survival surgery, where we injected KPC luciferase cells to generate PanCa tumor.

The *in vivo* results demonstrated that SPION-CUR-MUC13 and combination of CTLA-4 enhanced immunotherapy approach in C57BL/6 mice model. It has been observed that SPION-CUR-MUC13 formulation retained in the tumor and stromal area in mice body by Prussian blue staining (Fig. 26.). Tumor volume was efficiently controlled in SPION-CUR-MUC13 and combination with anti-PDL-1 and anti-CTLA-4 treated groups. Also, effectively enhanced the rate of survival in these treated groups when compared to monotherapy (Fig. 22.). This was supported with bioluminescent imaging of tumor (Fig. 21) and immune profiling through flow cytometry (Fig. 23. & 24.). The data from flow cytometry confirms the effects of SP-CUR-M13 on immune checkpoint expression on myeloid cells and thus provide the rationale for combination treatment with PD-L1/CTLA4 immune checkpoint blockade. Additionally, reduced immune tolerance, increased infiltration of total T cell population and CD8+T cells are observed

in mice treated with combination immune checkpoint therapy. The CTLA-4 combo treatment, in particular, resulted in a considerable reduction in tumor size in excised tumor tissues, as well as a greater survival rate (Fig. 22).

5. CONCLUSION

In conclusion, results indicate high therapeutic significance of MUC13-SPIONS for achieving targeted pancreatic tumor specific delivery of therapeutics. Since SPION-Curcumin particles inhibit the fibrotic immune tumor microenvironment, therefore, MUC13 conjugated SPION-curcumin can potentiate checkpoint immunotherapies, inhibit tumor growth and its progression. SPION-CUR-MUC13, when combined with CTLA-4, boosted T-cell infiltrates while reducing immunosuppressors. This SPION-CUR combination softened the tumor and strengthened immune checkpoint therapy.

REFERENCES

Adamska, A., Domenichini, A., & Falasca, M. (2017). Pancreatic Ductal Adenocarcinoma: Current and Evolving Therapies. *International Journal of Molecular Sciences, 18*(7), 1338. Retrieved from https://www.mdpi.com/1422-0067/18/7/1338

Aggarwal, B. B., Sundaram, C., Malani, N., & Ichikawa, H. (2007). Curcumin: the Indian solid gold. *The molecular targets and therapeutic uses of curcumin in health and disease*, 1-75.

American Cancer Society. (2019a). Cancer statistics for African Americans, 2019. *CA: a cancer journal for clinicians, 69*(3). Retrieved from https://acsjournals.onlinelibrary.wiley.com/doi/full/10.3322/caac.21555

American Cancer Society. (2019b). Surgery for Pancreatic Cancer,. Retrieved from https://www.cancer.org/cancer/pancreatic-cancer/treating/surgery.html

American Cancer Society. (2019c). What Is Pancreatic Cancer? Retrieved from https://www.cancer.org/cancer/pancreatic-cancer/about/what-is-pancreatic-cancer.html

American Cancer Society. (2020a). Chemotherapy for Pancreatic Cancer,. Retrieved from https://www.cancer.org/cancer/pancreatic-cancer/treating/chemotherapy.html

American cancer Society. (2020b). Tests for Pancreatic Cancer,. Retrieved from https://www.cancer.org/cancer/pancreatic-cancer/detection-diagnosis-staging/how-diagnosed.html

Apte, M. V., Wilson, J. S., Lugea, A., & Pandol, S. J. (2013). A starring role for stellate cells in the pancreatic cancer microenvironment. *Gastroenterology, 144*(6), 1210-1219. doi:10.1053/j.gastro.2012.11.037

Beatty, G. L., Winograd, R., Evans, R. A., Long, K. B., Luque, S. L., Lee, J. W., . . . Guirnalda, P. D. (2015). Exclusion of T cells from pancreatic carcinomas in mice is regulated by Ly6Clow F4/80+ extratumoral macrophages. *Gastroenterology, 149*(1), 201-210.

Biasci, D., Smoragiewicz, M., Connell, C. M., Wang, Z., Gao, Y., Thaventhiran, J. E. D., . . . Jodrell, D. I. (2020). CXCR4 inhibition in human pancreatic and colorectal cancers induces an integrated immune response. *Proc Natl Acad Sci U S A, 117*(46), 28960-28970. doi:10.1073/pnas.2013644117

Binnewies, M., Roberts, E. W., Kersten, K., Chan, V., Fearon, D. F., Merad, M., . . . Hedrick, C. C. (2018). Understanding the tumor immune microenvironment (TIME) for effective therapy. *Nature medicine, 24*(5), 541-550.

Boyiadzis, M. M., Kirkwood, J. M., Marshall, J. L., Pritchard, C. C., Azad, N. S., & Gulley, J. L. (2018). Significance and implications of FDA approval of pembrolizumab for biomarker-defined disease. *Journal for immunotherapy of cancer, 6*(1), 1-7.

Capasso, M., Franceschi, M., Rodriguez-Castro, K. I., Crafa, P., Cambiè, G., Miraglia, C., . . . Di Mario, F. (2018). Epidemiology and risk factors of pancreatic cancer. *Acta bio-medica : Atenei Parmensis, 89*(9-S), 141-146. doi:10.23750/abm.v89i9-S.7923

ClinicalTrials.gov. combination of immune checkpoint therapies | Active, not recruiting, Completed Studies | pancreatic cancer. Retrieved from https://clinicaltrials.gov/ct2/results?term=combination+of+immune+checkpoint+therapies&cond=pancreatic+cancer&Search=Apply&recrs=d&recrs=e&age_v=&gndr=&type=&rslt=

Feig, C., Gopinathan, A., Neesse, A., Chan, D. S., Cook, N., & Tuveson, D. A. (2012). The pancreas cancer microenvironment. *Clinical cancer research, 18*(16), 4266-4276.

Grivennikov, S. I., Greten, F. R., & Karin, M. (2010). Immunity, inflammation, and cancer. *Cell, 140*(6), 883-899.

Hruban, R. H., Adsay, N. V., Albores–Saavedra, J., Compton, C., Garrett, E. S., Goodman, S. N., . . . Longnecker, D. S. (2001). Pancreatic intraepithelial neoplasia: a new nomenclature and classification system for pancreatic duct lesions. *The American journal of surgical pathology, 25*(5), 579-586.

Hu, J.-X., Zhao, C.-F., Chen, W.-B., Liu, Q.-C., Li, Q.-W., Lin, Y.-Y., & Gao, F. (2021). Pancreatic cancer: A review of epidemiology, trend, and risk factors. *World journal of gastroenterology, 27*(27), 4298-4321. doi:10.3748/wjg.v27.i27.4298

Jaggi, M., Rao, P. S., Smith, D. J., Wheelock, M. J., Johnson, K. R., Hemstreet, G. P., & Balaji, K. (2005). E-cadherin phosphorylation by protein kinase D1/protein kinase Cμ is associated with altered cellular aggregation and motility in prostate cancer. *Cancer research, 65*(2), 483-492.

Johns Hopkins Medicine Pathology. (2021). Classification of ductal lesion in pancreas Retrieved from https://pathology.jhu.edu/pancreas/medical-professionals/duct-lesions

Kamath, S. D., Kalyan, A., Kircher, S., Nimeiri, H., Fought, A. J., Benson III, A., & Mulcahy, M. (2020). Ipilimumab and gemcitabine for advanced pancreatic cancer: a phase Ib study. *The oncologist, 25*(5), e808.

Khan, S., Chauhan, N., Yallapu, M. M., Ebeling, M. C., Balakrishna, S., Ellis, R. T., . . . Zafar, N. (2015). Nanoparticle formulation of ormeloxifene for pancreatic cancer. *Biomaterials, 53*, 731-743.

Khan, S., Ebeling, M. C., Zaman, M. S., Sikander, M., Yallapu, M. M., Chauhan, N., . . . Chauhan, S. C. (2014). MicroRNA-145 targets MUC13 and suppresses growth and

invasion of pancreatic cancer. *Oncotarget, 5*(17), 7599-7609. doi:10.18632/oncotarget.2281

Khan, S., Setua, S., Kumari, S., Dan, N., Massey, A., Hafeez, B. B., . . . Chauhan, S. C. (2019). Superparamagnetic iron oxide nanoparticles of curcumin enhance gemcitabine therapeutic response in pancreatic cancer. *Biomaterials, 208*, 83-97. doi:10.1016/j.biomaterials.2019.04.005

Khan, S., Zafar, N., Khan, S. S., Setua, S., Behrman, S. W., Stiles, Z. E., . . . Chauhan, S. C. (2018). Clinical significance of MUC13 in pancreatic ductal adenocarcinoma. *HPB (Oxford), 20*(6), 563-572. doi:10.1016/j.hpb.2017.12.003

Kota, J., Hancock, J., Kwon, J., & Korc, M. (2017). Pancreatic cancer: Stroma and its current and emerging targeted therapies. *Cancer Lett, 391*, 38-49. doi:10.1016/j.canlet.2016.12.035

Lafaro, K. J., & Melstrom, L. G. (2019). The paradoxical web of pancreatic cancer tumor microenvironment. *The American journal of pathology, 189*(1), 44-57.

Li, W., Sun, L., Lei, J., Wu, Z., Ma, Q., & Wang, Z. (2020). Curcumin inhibits pancreatic cancer cell invasion and EMT by interfering with tumor□stromal crosstalk under hypoxic conditions via the IL□6/ERK/NF□κB axis. *Oncology reports, 44*(1), 382-392.

Maher, D. M., Gupta, B. K., Nagata, S., Jaggi, M., & Chauhan, S. C. (2011). Mucin 13: structure, function, and potential roles in cancer pathogenesis. *Molecular Cancer Research, 9*(5), 531-537.

Malhotra, L., Ahn, D., & Bloomston, M. (2015). The pathogenesis, diagnosis, and management of pancreatic cancer. *J Gastrointest Dig Syst, 5*(2), 1-11.

Mashayekhi, V., Mocellin, O., Fens, M. H. A. M., Krijger, G. C., Brosens, L. A. A., & Oliveira, S. (2021). Targeting of promising transmembrane proteins for diagnosis and treatment of pancreatic ductal adenocarcinoma. *Theranostics, 11*(18), 9022-9037. doi:10.7150/thno.60350

Mocci, E., Kundu, P., Wheeler, W., Arslan, A. A., Beane-Freeman, L. E., Bracci, P. M., . . . Gallinger, S. (2021). Smoking modifies pancreatic cancer risk loci on 2q21. 3. *Cancer research, 81*(11), 3134-3143.

National Cancer Institute. (2018). FOLFIRINOX,. Retrieved from https://www.cancer.gov/about-cancer/treatment/drugs/folfirinox#:~:text=FOLFIRINOX%20is%20used%20to%20treat%3A%20Pancreatic%20cancer%20that,scientific%20definition%20and%20other%20names%20for%20this%20drug.

Oberstein, P. E., & Olive, K. P. (2013). Pancreatic cancer: why is it so hard to treat? *Therapeutic advances in gastroenterology, 6*(4), 321-337. doi:10.1177/1756283X13478680

Pardoll, D. M. (2012). The blockade of immune checkpoints in cancer immunotherapy. *Nature Reviews Cancer, 12*(4), 252-264.

Peer, D., Karp, J. M., Hong, S., Farokhzad, O. C., Margalit, R., & Langer, R. (2007). Nanocarriers as an emerging platform for cancer therapy. *Nature nanotechnology, 2*(12), 751-760.

Pham, T. N., Shields, M. A., Spaulding, C., Principe, D. R., Li, B., Underwood, P. W., . . . Munshi, H. G. (2021). Preclinical Models of Pancreatic Ductal Adenocarcinoma and Their Utility in Immunotherapy Studies. *Cancers, 13*(3), 440.

Qu, C., Wang, Q., Meng, Z., & Wang, P. (2018). Cancer-associated fibroblasts in pancreatic cancer: should they be deleted or reeducated? *Integrative cancer therapies, 17*(4), 1016-1019.

Saif, M. W. (2013). US Food and Drug Administration approves paclitaxel protein-bound particles (Abraxane®) in combination with gemcitabine as first-line treatment of patients with metastatic pancreatic cancer. *JOP. Journal of the Pancreas, 14*(6), 686-688.

SEER. (2021). Cancer Stat Facts: Pancreatic Cancer,. Retrieved from https://seer.cancer.gov/statfacts/html/pancreas.html#:~:text=Pancreatic%20cancer%20is%20the%20third%20leading%20cause%20of,cancer%20deaths%20is%20highest%20among%20people%20aged%2065%E2%80%9374.

Siegel, R. L., Miller, K. D., & Jemal, A. (2016). Cancer statistics, 2016. *CA: a cancer journal for clinicians, 66*(1), 7-30.

Sung, H., Ferlay, J., Siegel, R. L., Laversanne, M., Soerjomataram, I., Jemal, A., & Bray, F. (2021). Global cancer statistics 2020: GLOBOCAN estimates of incidence and mortality worldwide for 36 cancers in 185 countries. *CA: a cancer journal for clinicians, 71*(3), 209-249.

Swann, J. B., & Smyth, M. J. (2007). Immune surveillance of tumors. *The Journal of clinical investigation, 117*(5), 1137-1146.

Teng, C., Zhang, B., Yuan, Z., Kuang, Z., Chai, Z., Ren, L., . . . Yin, L. (2020). Fibroblast activation protein-α-adaptive micelles deliver anti-cancer drugs and reprogram stroma fibrosis. *Nanoscale, 12*(46), 23756-23767.

Wainberg, Z. A., Hochster, H. S., Kim, E. J., George, B., Kaylan, A., Chiorean, E. G., . . . Jain, R. (2020). Open-label, phase I study of nivolumab combined with nab-paclitaxel plus gemcitabine in advanced pancreatic cancer. *Clinical cancer research, 26*(18), 4814-4822.

Weiss, G. J., Blaydorn, L., Beck, J., Bornemann-Kolatzki, K., Urnovitz, H., Schütz, E., & Khemka, V. (2018). Phase Ib/II study of gemcitabine, nab-paclitaxel, and pembrolizumab in metastatic pancreatic adenocarcinoma. *Investigational new drugs, 36*(1), 96-102.

Wu, A. A., Bever, K. M., Ho, W. J., Fertig, E. J., Niu, N., Zheng, L., . . . Ferguson, A. K. (2020). A Phase II study of allogeneic GM-CSF–transfected pancreatic tumor vaccine (GVAX) with ipilimumab as maintenance treatment for metastatic pancreatic cancer. *Clinical cancer research, 26*(19), 5129-5139.

Yallapu, M. M., Ebeling, M. C., Khan, S., Sundram, V., Chauhan, N., Gupta, B. K., . . . Chauhan, S. C. (2013). Novel curcumin-loaded magnetic nanoparticles for pancreatic cancer treatment. *Mol Cancer Ther, 12*(8), 1471-1480. doi:10.1158/1535-7163.Mct-12-1227

Yallapu, M. M., Othman, S. F., Curtis, E. T., Bauer, N. A., Chauhan, N., Kumar, D., . . . Chauhan, S. C. (2012). Curcumin-loaded magnetic nanoparticles for breast cancer therapeutics and imaging applications. *International journal of nanomedicine, 7*, 1761.

Yallapu, M. M., Othman, S. F., Curtis, E. T., Gupta, B. K., Jaggi, M., & Chauhan, S. C. (2011). Multi-functional magnetic nanoparticles for magnetic resonance imaging and cancer therapy. *Biomaterials, 32*(7), 1890-1905.

Yoon, J. H., Jung, Y.-J., & Moon, S.-H. (2021a). Immunotherapy for pancreatic cancer. *World journal of clinical cases, 9*(13), 2969.

Yoon, J. H., Jung, Y.-J., & Moon, S.-H. (2021b). Immunotherapy for pancreatic cancer. *World journal of clinical cases, 9*(13), 2969-2982. doi:10.12998/wjcc.v9.i13.2969

Young, K., Hughes, D. J., Cunningham, D., & Starling, N. (2018). Immunotherapy and pancreatic cancer: unique challenges and potential opportunities. *Therapeutic advances in medical oncology, 10*, 1758835918816281.

Zhang, L., Sanagapalli, S., & Stoita, A. (2018). Challenges in diagnosis of pancreatic cancer. *World journal of gastroenterology, 24*(19), 2047.

Zhou, Q., Tao, X., Xia, S., Guo, F., Pan, C., Xiang, H., & Shang, D. (2020). T Lymphocytes: A Promising Immunotherapeutic Target for Pancreatitis and Pancreatic Cancer? *Front Oncol, 10*, 382. doi:10.3389/fonc.2020.00382

APPENDIX

APPENDIX

1. TABLES

Table 1.

Table 1: Weight of SPION Particle after Lyophilization				
Sample	**1**	**2**	**3**	**Average**
Empty tube	1.5237g	1.5395 g	1.5357 g	-
After Lyophilization	1.5311 g	1.5464 g	1.5426 g	-
Weight	7.4 mg	6.9 mg	6.9 mg	7.06 mg

Table 2.

Table 2: Characterization of SPION using Malvern Zetasizer Ultra				
	Read 1	**Read 2**	**Read 3**	**Total Average**
Size (Z Average nm)	96.04	97.38	96.87	96.76 nm
Charge (Zeta potential mV)	-28.31	-24.54	-24.8	-25.8833 mV

Table 3.

Table 3: Characterization of SPION-CUR using Malvern Zetasizer Ultra				
	Read 1	**Read 2**	**Read 3**	**Total Average**
Size (Z Average nm)	114.9	114.9	118	115.9 nm
Charge (Zeta potential mV)	-21.06	-20.19	-22.92	-21.39 mV

Table 4.

Table 4: Tumor Size by gram			
Treatments	**Tumor %**	**Weight (gram)**	**SEM**
SP	93.28037	2.2383	0.545006
SP-CUR-Ig	83.9302	2.01394	0.250631
SP-Cur-M13	93.9096	2.2534	0.247581
PDL-1	100	2.39954	0.362806
CTLA-4	42.1364	2.2301	0.520324
SP-Cur-M13 + PDL-1	92.9386	1.01108	0.32479
SP-Cur-M13 + CTLA-4	28.4804	0.84584	0.277978

Table 5.

Table. 5 Number of deaths each week with respect to each group							
	23-Aug	30-Aug	6-Sep	13-Sep	20-Sep	27-Sep	Total mice
	Week 1	**Week 2**	**Week 3**	**Week 4**	**Week 5**	**Week 6**	
SPION	0	3	2	0	0	0	5
SPION-CUR-Ig	0	3	2	0	0	0	5
SPION-CUR-MUC13	0	1	3	1	0	0	5
PDL-1	0	1	2	2	0	0	5
CTLA-4	0	2	2	1	0	0	5
SPION-CUR-MUC13 + PDL-1	0	1	3	1	0	0	5
SPION-CUR-MUC13 + CTLA-4	0	0	2	0	1	2(survived)	5

Table 6.

Table. 6 Recorded Death Date per week with respect to each group				
Group	**Treatment**	**Death Date**	**Number of mice**	**Weeks**
-	-	-	null	Week 1 (23-Aug)
1	SPION	8/31/2021	one	Week 2 (30-Aug)
1	SPION	8/31/2021	one	
5	CTLA-4	9/1/2021	one	
2	SPION-CUR-IgG	9/3/2021	one	
5	CTLA-4	9/3/2021	one	
4	PDL-1	9/3/2021	one	
1	SPION	9/4/2021	one	
6	SPION-CUR-MUC13 +PDL-1	9/4/2021	one	
2	SPION-CUR-IgG	9/4/2021	two	
3	SPION-CUR-MUC13	9/5/2021	one	
4	PDL-1	9/6/2021	one	Week 3 (6-Sep)
7	SPION-CUR-MUC13 +CTLA-4	9/6/2021	one	
3	SPION-CUR-MUC13	9/6/2021	one	
5	CTLA-4	9/6/2021	one	
3	SPION-CUR-MUC13	9/7/2021	one	
1	SPION	9/7/2021	one	

2	SPION-CUR-IgG	9/7/2021	one	
6	SPION-CUR-MUC13 +PDL-1	9/7/2021	two	
3	SPION-CUR-MUC13	9/8/2021	one	
4	PDL-1	9/8/2021	one	
1	SPION	9/9/2021	one	
6	SPION-CUR-MUC13 +PDL-1	9/10/2021	one	
2	SION-CUR-IgG	9/10/2021	one	
7	SPION-CUR-MUC13 +CTLA-4	9/11/2021	one	
5	CTLA-4	9/11/2021	one	
3	SPION-CUR-MUC13	9/13/2021	one	Week 4 (13-Sep)
5	CTLA-4	9/13/2021	one	
4	PDL-1	9/13/2021	two	
6	SPION-CUR-MUC13 + PDL-1	9/17/2021	one	
7	SPION-CUR-MUC13 + CTLA-4	9/20/2021	one	Week 5 (20-Sep)
7	SPION-CUR-MUC13 +CTLA-4	9/27/2021	Sacrificed two	Week 6 (27-Sep)

BIOGRAPHICAL SKETCH

Poornima Devi Shaji, is an Indian native. She graduated from the SRM Institute of Science and Technology at Chennai, India in 2018 with a Bachelor of Technology in Genetic Engineering. While studying at SRM, she was introduced to Dr. Rashmi Mishra's Lab, Division of Neurobiophysics, Rajiv Gandhi Centre for Biotechnology for her bachelor's dissertation. The work done with Dr. Rashmi Mishra's lab led her to the discipline of Cancer, where she evaluated the efficacy of the extract of *Emblica Officinalis* in inhibition of Tumor progression in cervical cancer cell line. After her graduation, she worked as Project Technical Assistant in 2019, at Cutaneous, Cancer and Ayurveda Biology Research Lab, Dept. of Zoology, University of Kerala, Trivandrum, India.

She completed her Master of Science degree in Biochemistry and Molecular Biology in December 2021. She continued the discipline of cancer with master's thesis. The research was done under the supervision of Dr. Subhash Chauhan and Dr. Sheema Khan, Department of Immunology and Microbiology, School of Medicine, University of Texas Rio Grande Valley. She developed a novel strategy to improve checkpoint immune response in pancreatic cancer. She has awarded with Biochemistry and Molecular Biology Master's program Graduate Research Assistantship (BCMB MS GRA) and Graduate Teaching Assistantship (GTA) from School of Science, University of Texas Rio Grande Valley, Edinburg, Texas. She can be reached at personal email address poornimadevis97@gmail.com